sustainability

MDPI

Article

Effects of Lake–Reservoir Pumped-Storage Operations on Temperature and Water Quality

Ulrike Gabriele Kobler [1,*], Alfred Wüest [1,2] and Martin Schmid [1]

[1] Eawag, Swiss Federal Institute of Aquatic Science and Technology, Surface Waters—Research and Management, CH-6047 Kastanienbaum, Switzerland; alfred.wueest@eawag.ch (A.W.); martin.schmid@eawag.ch (M.S.)

[2] EPFL, Physics of Aquatic Systems Laboratory—Margaretha Kamprad Chair, ENAC-IEE-APHYS, CH-1015 Lausanne, Switzerland

* Correspondence: ulrike.kobler@eawag.ch

Received: 14 May 2018; Accepted: 8 June 2018; Published: 12 June 2018

Abstract: Pumped-storage (PS) hydropower plants are expected to make an important contribution to energy storage in the next decades with growing market shares of new renewable electricity. PS operations affect the water quality of the connected water bodies by exchanging water between them but also by deep water withdrawal from the upper water body. Here, we assess the importance of these two processes in the context of recommissioning a PS hydropower plant by simulating different scenarios with the numerical hydrodynamic and water quality model CE-QUAL-W2. For extended PS operations, the results show significant impacts of the water exchange between the two water bodies on the seasonal dynamics of temperatures, stratification, nutrients, and ice cover, especially in the smaller upper reservoir. Deep water withdrawal was shown to strongly decrease the strength of summer stratification in the upper reservoir, shortening its duration by ~ 1.5 months, consequently improving oxygen availability, and reducing the accumulation of nutrients in the hypolimnion. These findings highlight the importance of assessing the effects of different options for water withdrawal depths in the design of PS hydropower plants, as well as the relevance of defining a reference state when a PS facility is to be recommissioned.

Keywords: hydropower; stratification; reservoir modeling; recommissioning

1. Introduction

The share of "new renewables", such as photovoltaic and wind power plants, to the electricity production is increasing globally as a consequence of political decisions to reduce greenhouse gas emissions [1,2]. At the end of 2016, 2017 GW of renewable power capacity were installed globally [3], with parts of ~300 GW and ~490 GW from photovoltaic and wind power, respectively. The integration of these "new renewables" to the electrical grid is challenging due to their intermittency [4] and entails network load stability problems resulting from decentralized production [5]. Electricity storage addresses a large part of these timing and stability issues.

Even today, the most efficient technologies for storing electric energy are still pumped-storage (PS) hydropower plants, which also provide ancillary services such as voltage support and various forms of reserve capacity to fine-tune the matching of supply and demand and to ensure reliability [3]. Worldwide, >300 PS hydropower plants were installed with a total capacity of ~150 GW by the end of 2016, and plans existed for another 40 GW by 2020 [3], with overall energy efficiencies reaching up to 87% and an individual size of up to 3000 MW [6]. Thus, within the last few years, PS operations regained attention, and overviews of proposed PS hydropower plants have been presented in various studies [1,7].

However, PS operations modify physical and geochemical (abiotic) as well as ecological (biotic) properties of the connected water bodies. Abiotic effects include changes of water temperature, stratification, water level fluctuations, sediment resuspension, oxygen and nutrient cycling in the water column as well as modifications of inorganic suspended sediment, which accordingly alter light penetration [8]. Additionally, lake-internal circulation patterns [9] as well as ice cover [10,11] may be affected.

Biotic PS impacts are, in general, less studied but can include effects such as stranding of juvenile fish in littoral zones during dewatering [12], entrainment of organisms [13], and spreading of alien species from downstream to upstream [14].

Assessing PS impacts for different scenarios is typically undertaken by the application of numerical models. Models of different complexity have previously been applied for studying impacts of reservoir management on water quality. These range from one-dimensional models such as GLM-AED [15], DYRESM-CAEDYM [16] or MyLake [17], to three-dimensional models such as the Environmental Fluid Dynamics Code [18], Delft3D [19] or ELCOM-CAEDYM [16,20]. Models of lower complexity have the advantage of shorter computation times, allowing for large numbers of simulations, e.g., for the purpose of parameter estimation or scenario simulations, but may not be able to adequately reproduce the effects of local inflows on basin-scale dynamics and water quality, especially for large local discharges as they are typically introduced by PS operations. Three-dimensional models can resolve these spatial dynamics, but their computational demand, especially when coupled to water quality models, still precludes their application to long-term studies and for purposes where a large number of simulations is required. Furthermore, spatially resolved observational data are often not available to calibrate the three-dimensional processes.

For our case, the simulation of a coupled lake–reservoir system over a time scale of 15 years and with a potential future application to climate change scenarios, the two-dimensional, laterally averaged hydrodynamic and water quality model CE-QUAL-W2 is a good compromise between spatial resolution and computational demand. It has previously been applied to numerous case studies for reservoir management [21,22], among which also another case study of a lake and a reservoir coupled by PS [23].

When planning a new or extending an existing PS scheme, environmental effects need to be projected and minimized during the planning phase [14,24]. For this purpose, a reference state needs to be defined. This could be the natural state without a reservoir. However, in the case of existing reservoirs, which are often used for multiple purposes, such as for flood protection and recreation [14], reservoir removal could have relevant ecological and socio-economic effects, and might therefore not be a realistic option [25]. Hence, other artificial reference states can be considered to analyze the impacts of PS extension or for recommissioning present PS operation.

This study aimed to assess the impacts on temperature, stratification as well as water quality in a natural lake and a reservoir connected by a PS hydropower plant. We analyzed: (a) its extension; and (b) two reference scenarios without PS operation. Both reference scenarios keep the dam, but they differ in withdrawal depth of the outflow which either remains at the current depth of the residual flow outlet in the hypolimnion or is moved up to the surface. The first reference scenario allowed individually assessing the impacts of water exchange due to PS, while the second corresponded to a "quasi-natural" behavior of the reservoir. We hypothesized that the impacts of PS operations are partially caused by the exchange of water between the two water bodies, and partially by the depth of water removal from the upper reservoir. To disentangle these effects, the scenarios were simulated using the 2D-model CE-QUAL-W2 and compared to the present PS operation.

2. Study Site

Etzelwerk, a PS hydropower plant located in Switzerland, was chosen as the study site. It was built in the 1930s and is operated between Sihlsee and Upper Lake Zurich (Figure 1). Its current concession runs out at the end of 2022. For its renewal, several options for extending the PS operation

have been considered: 525 (265) MW, 250 (80) MW and 150 (60) MW for the generating (pumping) mode. Additionally, a reference state was defined as a base for the required mitigation measures.

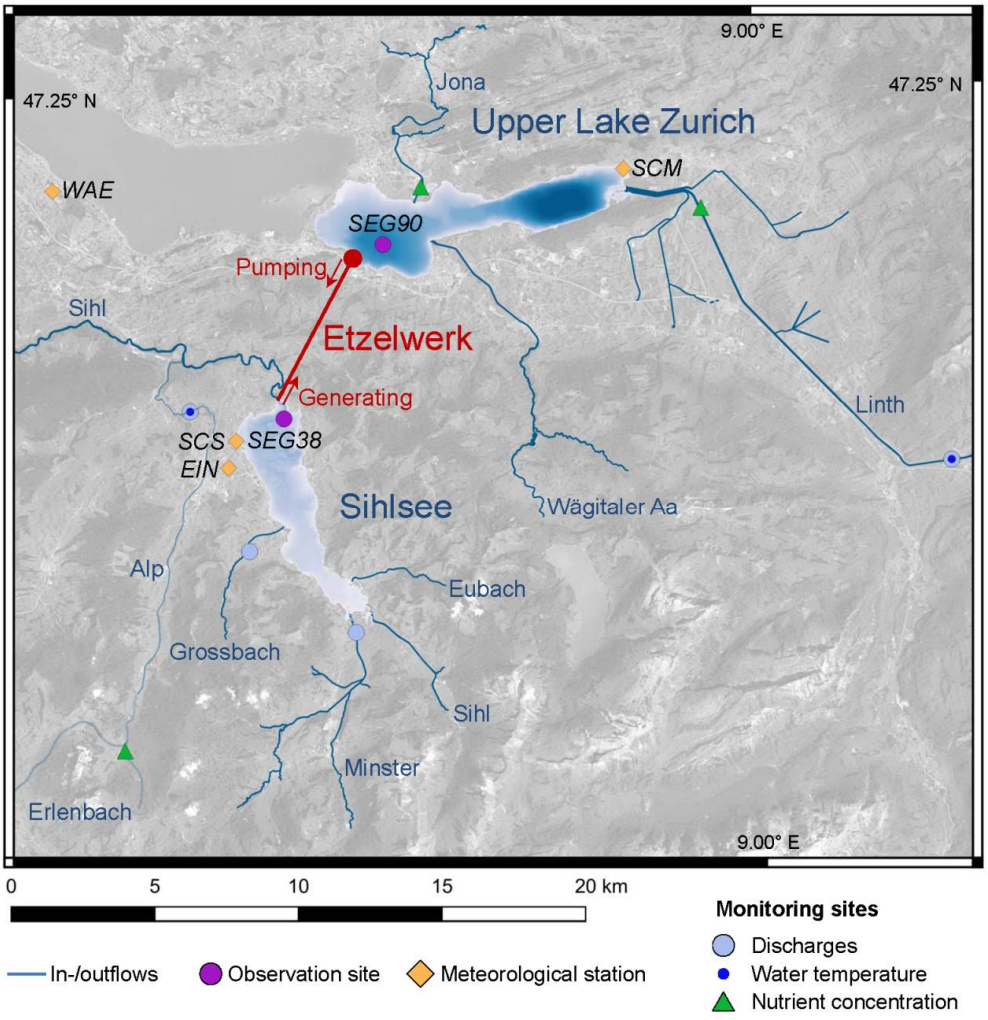

Figure 1. Overview of study site: Etzelwerk with its two connected water bodies Sihlsee (upper reservoir; 8.5 km long and 2.5 km wide) and Upper Lake Zurich (lower lake; 10.5 km long and 2.5 km wide). Meteorological stations refer to: EIN: Einsiedeln; WAE: Wädenswil; SCM: Schmerikon (all MeteoSwiss); and SCS: Segelclub Sihlsee. The MeteoSwiss station at Zurich Fluntern (SMA) is outside the graph (coordinates: 8.56573° E, 47.37789° N). Observation sites correspond with the deepest points of model segments 38 (SEG38) and 90 (SEG90), for which model results were generated.

Sihlsee is the artificial upper reservoir of the Etzelwerk PS hydropower plant (Figure 1). At maximum water level, it is 23 m deep, has a surface area of 11.3 km^2 and a volume of 96.1 $\times$ 10^6 m^3. The water level varies by 12.5 m between 889.34 and 876.84 m a.s.l., thus the storage capacity is ~89.4 $\times$ 10^6 m^3. The catchment area is 156.5 km^2, with the major tributaries Minster (40% of catchment), Sihl (21%), Grossbach (7%) and Eubach (6%). The grid location of inflows, outflows and PS flows is depicted in Figure A1 of Supplementary Material S1. The current hydraulic residence time is ~135 days. Since no previous observations were available, temperature, oxygen and nutrient concentrations were monitored in Sihlsee during 2014–2016 as a base for model calibration. The observations were made at SEG38 and are summarized in Supplementary Material S1 (Section B).

Upper Lake Zurich is the lower lake of this PS hydropower plant and is of natural origin (Figure 1). Its surface elevation varies by ~1.0 m between 405.5 and 406.5 m a.s.l. At highest water level, it has a maximum depth of 48 m, a surface area of 20.25 km^2 and a volume of 470 $\times$ 10^6 m^3. The catchment

area (1564 km^2) is about one order of magnitude larger than that of Sihlsee. The main tributaries contributing to this catchment are Linth (83%, including the discharge from Walensee and Linthebene), Jona (5%) and Wägitaler Aa (5%). The average water residence time is ~70 days. Additional information on bathymetry and model forcing can be found in Supplementary Material S1 (Section A), and an overview of the physical and chemical properties of Upper Lake Zurich (monitored by a routine program at SEG90) is given in Supplementary Material S1 (Section B).

Epilimnion temperatures at both lakes are rather similar. Hypolimnion temperatures at Sihlsee can reach up to <17 °C in summer, whereas those at Upper Lake Zurich remain below 6 °C. During the stagnation phase, suboxic or anoxic conditions develop in the hypolimnia of both lakes. Mean annual nitrate concentrations differ significantly between Sihlsee (~230 µg N L^{-1}) and Upper Lake Zurich (~660 µg N L^{-1}), respectively, while mean total phosphorus concentrations are similar in both water bodies, even though higher peak concentrations are reached in Sihlsee after flood events.

The average annual water balances (calculated for the period 1997–2015) of both water basins are given in Table 1. The extended PS operation would increase the water exchange between the two water bodies from 214 to 778 m^3 s^{-1} for the PS generating flow and from 26 to 590 m^3 s^{-1} for the PS pumping flow (Table 1). The seasonality of the artificial PS flows is shown in Figure A2 of Supplementary Material S1. For both reference scenarios, no PS flows were considered. The hydraulic residence time of Sihlsee is, therefore, increased to ~150 days in both reference scenarios and reduced to ~40 days in the extended PS scenario.

Table 1. Annual water balance of the two water bodies of Etzelwerk. Sum of all inflows, outflows and artificial flows for present and extended PS operation as well as for the two reference scenarios NoPS and QNat (details given in Section 3.2). A correction term was required to close the water balance for Sihlsee, described in Supplementary Material S1 (Section A.3).

	Sihlsee			Upper Lake Zurich		
	Present PS	**Extended PS**	**Reference Scenarios**	**Present PS**	**Extended PS**	**Reference Scenarios**
			[10^6 m^3 $year^{-1}$]			
Sum of inflows	235	235	235	2410	2410	2410
Sum of outflows	−32	−32	−220	−2598	−2598	−2410
Correction term	−15	−15	−15	0	0	0
PS generating flow	−214	−778	0	214	778	0
PS pumping flow	26	590	0	−26	−590	0

3. Materials and Methods

3.1. Model Description

The simulations were run with the model CE-QUAL-W2, version 3.71 [26], developed in a cooperation of the US Corps of Engineers and the Portland State University. It is a two-dimensional laterally averaged hydrodynamic and water quality model. The two water bodies are directly connected in the model, i.e., the volumes of head race tunnel and penstock are neglected. In effect, this volume needs to be flushed at every PS flow inversion before water is effectively transferred between the two water bodies. For the present PS, this accounts for ~5% and ~13% of the generating and pumping flows, respectively. Thus, the volume exchanged between the two water bodies is slightly overestimated. Frictional losses were considered, with an assumption of 90% and 80% efficiency level for generating and pumping, respectively. The effect of this frictional warming was, however, minor.

The model forcing includes meteorological, hydrological and water quality forcing as well as bathymetrical data. A detailed description including initial conditions is given in Supplementary Material S1 (Section A). All simulations were run for the period 1997–2012, whereas years 2013–2015 and 1998–2015 were used for calibration of Sihlsee and Upper Lake Zurich, respectively. The first year of each period was considered as spin-up phase, and not included in the results. The results shown for Sihlsee were generated at model segment 38 (SEG38), and those for Upper Lake Zurich at model

segment 90 (SEG90) (Figure 1). These segments correspond to the observation locations at the two water bodies. A detailed description of the PS scenarios follows in Section 3.2.

The model considered an hourly time step and the model variables comprise: water temperature, dissolved oxygen, inorganic suspended solids, phosphate, ammonium, sum of nitrate and nitrite, dissolved and particulate organic matter (labile and refractory), algae (two groups) and zooplankton.

The model was calibrated against observations through a manual trial and error calibration. Parameter values were either set according to recommendations from literature or tuned to match observations (details in Supplementary Material S1: Section B). The identified parameter set, the comparison between observed and simulated profiles and time series as well as the computed mean absolute error (MAE) and mean error (ME) of temperature, dissolved oxygen, total phosphorus and the sum of nitrate and nitrite are given in Supplementary Material S1 (Section B.2).

The root mean square errors (RMSEs) for the entire calibration period for the overall water column, the epilimnion and the hypolimnion are shown in Table 2. The RMSE of temperature is <1 °C for both water bodies, which is comparable to the range of ~0.7–2.1 °C achieved in a recent multi-lake comparative analyses using the 1D-model GLM [27]. The MAEs (Table B1 of Supplementary Material S1) for the entire water column of 0.71 °C for Sihlsee and 0.65 °C for Upper Lake Zurich are within the range of ~0.3–0.9 °C that resulted from 70 previous applications of CE-QUAL-W2 [26]. RMSEs for dissolved oxygen are comparable to the value of 1.05 mg L^{-1} in a recent study on reducing thermal pollution downstream with the additional objective to avoid hypoxia [15], and again within the range typically achieved with CE-QUAL-W2 for similar applications [26,28]. The same is true for nutrient concentrations, where, for example, Deliman and Gerald [28] showed RMSEs of 570 µg N L^{-1} for the sum of nitrate and nitrite and 40 µg P L^{-1} for total phosphorus; and Smith et al. [29] presented RMSEs in the hypolimnion of ≤100 µg N L^{-1} for the sum of nitrate and nitrite and ≤16 µg P L^{-1} for total phosphorus as well as RMSEs in the epilimnion of ≤40 µg N L^{-1} and ≤7 µg P L^{-1} for the sum of nitrate and nitrite and total phosphorus, respectively. RMSEs of the sum of nitrate and nitrite presented in two further studies, which both focussed on projecting the response to nutrient reduction scenarios, were ~100 µg N L^{-1} for both epi- and hypolimnion [22] and ≤590 µg N L^{-1} [21] for the entire water column.

Table 2. Root mean square error (RMSE) of temperature, dissolved oxygen, the sum of nitrate and nitrite as well as total phosphorus computed for the entire water column, the epilimnion and the hypolimnion of Sihlsee and Upper Lake Zurich.

		Sihlsee			Upper Lake Zurich		
		2014–2015			1998–2015		
Variable	**Unit**	**Entire Water Column**	**Epilimnion [1]**	**Hypolimnion [2]**	**Entire Water Column**	**Epilimnion [1]**	**Hypolimnion [3]**
Temperature	[°C]	0.94	0.93	0.94	0.93	0.78	0.98
Dissolved oxygen	[mg L^{-1}]	1.15	1.07	1.38	1.26	0.99	1.16
Sum nitrate and nitrite	[µg N L^{-1}]	76	69	89	114	142	114
Total phosphorus	[µg P L^{-1}]	4.45	2.74	6.51	4.13	3.90	3.96

[1] Uppermost 5 m of the water column. [2] Lowermost 5 m of the water column. [3] All depths ≤20 m.

3.2. Pumped-Storage Scenarios

Here, we present the results of simulations corresponding to present PS operations, the largest PS extension scenario and two reference scenarios considering no PS flows.

The present PS scenario represents the current state, where water is withdrawn from the hypolimnion of Sihlsee for both generating electricity (~135 MW installed capacity) and the residual flow to River Sihl. Water from Upper Lake Zurich is pumped up to Sihlsee (~65 MW installed capacity)

and discharged to its hypolimnion. At Upper Lake Zurich, intake and outlet of the PS hydropower plant are placed within the epilimnion.

The extended PS is operated with installed capacities of 525 MW and 265 MW for generating and pumping, respectively. The basic hourly dataset for this scenario was provided by the Swiss Federal Railways and considered monthly-averaged net inflows to Sihlsee. It was adapted to account for hourly instead of monthly mean natural inflows, to allow assessing the influence of floods and low flows (details are given in Section A.3 of Supplementary Material S1).

For the first reference scenario (NoPS) water is withdrawn from the hypolimnion through the present outlet of River Sihl's residual flow. The discharge of River Sihl downstream the dam is based on a regime analysis of observed outflows, before the dam was built (LIMNEX AG, 2016, personal communication), representing a near-natural effluent for River Sihl downstream of the dam.

For the second reference scenario (QNat), the discharge to River Sihl is similar to that of NoPS, but released from the epilimnion, where water is discharged over a weir (crest at 887.4 m a.s.l., of Figure A1 Supplementary Material S1). This outflow corresponds to the "theoretical" natural state of the lake, if the dam were of natural origin.

The current PS generating flow approximately equals the sum of inflows for Sihlsee, but contributes <10% to the total inflows of Upper Lake Zurich (Table 1). The pumping flow accounts for ~10% of the natural inflows at Sihlsee and for ~1% at Upper Lake Zurich. Consequently, the impacts of the PS operations are much more important for Sihlsee, and we focus the discussion of the results on this reservoir. Results for Upper Lake Zurich are presented in Supplementary Material S1 (Section C).

3.3. Aggregation of Results

From the simulated temperatures and concentrations of dissolved oxygen and nutrients, we calculated means, minima and maxima of all years included in the studied period (1998–2012) for each day of the year. The simulations were aggregated separately for the epilimnion (represented by the uppermost 5 m of the water column) and the hypolimnion (represented by the lowermost 5 m of the water column). The differences between scenarios were calculated at every depth and then aggregated for either the epi- or the hypolimnion. The aggregation included the computation of mean and standard deviation for each season.

The durations of summer and inverse winter stratification were defined as the longest uninterrupted periods with temperature differences >0.2 °C and <−0.2 °C between the upper- and the lowermost layer. Schmidt stability was calculated according to Idso [30] for each day and its mean value was calculated for each month. Ice-on was defined as the first day in winter, when ice thickness at SEG38 was >0 m, and ice-off as the first day in spring without ice at SEG38.

4. Results

Figure 2 depicts the mean and extrema for temperature, dissolved oxygen and nutrients for all considered PS scenarios, and Figure 3 shows a boxplot of their seasonal differences between either one of the two reference scenarios QNat and NoPS or the extended PS scenario and the present PS scenario. In both figures, the results are presented separately for the epi- and the hypolimnion.

In summer and autumn (May–December), epilimnion temperatures of Sihlsee are ~1.6 °C lower in the reference scenario QNat compared to all other scenarios. Hypolimnion temperatures for QNat are reduced by up to 10–11 °C in late August compared to the other scenarios. These large temperature differences result from hypolimnetic water withdrawal, which draws the thermocline and warmer epilimnion water downwards. This highlights the strong effect of deep water withdrawal on the temperature regime of Sihlsee. In contrast, the hypolimnion temperature differences between the extended and the present PS operation generally range within ~3 °C, and those between the present PS operation and NoPS are <1 °C for most of the summer. In both cases, the hypolimnion of Sihlsee is warmed during summer due to pumping of epilimnion water from Upper Lake Zurich.

In winter and spring (December–May), epilimnetic temperatures are similar for all scenarios except for the extended PS scenario, where they increase by ~1.6 °C. These differences are shaped by enhanced PS pumping flow during winter and result also in a significantly shortened ice-covered period (Figure 4a) along with start and end dates of summer and inverse stratification, for the extended PS scenario. This further results in a decreasing ice thickness from ~30–34 cm to ~23 cm for the extended PS scenario (Figure 4c). Inverse stratification is also shortened by ~50 days (later start and earlier end) due to the pumping of comparably warm water from Upper Lake Zurich.

The deep water withdrawal of present PS, extended PS and NoPS reference scenarios affects stratification (Figure 4a) and water column stability (Figure 4b) accordingly. Summer stratification is prolonged for QNat by ~40–50 days since water temperatures are much cooler for this scenario in autumn and more time is needed to cool the water column sufficiently to initiate mixing. For extended PS, summer stratification is prolonged by ~10–15 days, caused by earlier stratification start due to earlier ice-off (Figure 4a).

Schmidt stability is for most months smallest in the extended PS scenario (Figure 4b). Thus, enhanced PS pumping flow generally decreases water column stability. In the simulations this leads occasionally (three times in 12 years) to temperature differences <0.5 °C between the upper- and lowermost layer, and, thus, strong wind events can initiate almost complete mixing of the water column in summer. This does not occur in the near-natural reference scenario QNat. The other three scenarios show major differences from August to October, where Schmidt stability is decreased by factors of up to ~3.3 compared to the reference scenario QNat.

Dissolved oxygen concentrations in the epilimnion are mainly driven by equilibration with the atmosphere and primary production and do not differ much between the scenarios, only the shorter ice-covered period slightly raises concentrations in spring for the extended PS scenario. Conversely, large differences arise in the hypolimnion, where the prolonged stratification in the reference scenarios QNat increases the time available for oxygen depletion due to the decomposition of organic matter. This leads to maximum differences of ~8 mg L^{-1} in late October when hypolimnetic oxygen concentrations reach their minimum in QNat, but are already partially replenished by seasonal mixing in the other scenarios. In addition, PS introduces oxygen-rich water from the epilimnion of Upper Lake Zurich to the hypolimnion of Sihlsee, counteracting oxygen depletion during both summer stratification and inverse winter stratification, which is particularly the case for the extended PS scenario (Figure 3). Following the Swiss Water Protection Ordinance [31], dissolved oxygen concentrations in lakes should always exceed a threshold of 4 mg L^{-1}. In the near-natural reference scenario QNat, simulated concentrations fall below this threshold every year, on average during ~90 days. This value is reduced to ~33 days (in 14 out of 15 years) for the reference NoPS, and ~22 days (11 years) for the present PS scenario. For the extended PS scenario, hypolimnetic dissolved oxygen concentrations below 4 mg L^{-1} were simulated only in one year for an uninterrupted period of ~3 days, which is still less than for the other scenarios in that specific year.

Nutrient concentrations are also affected by both the exchange of water in the PS scenarios and the changes in stratification due to the withdrawal depth. The sum of nitrate and nitrite concentrations is increased by a factor of ~1.2–4 in the extended PS scenario, as the prevailing concentrations are higher by factor of ~3 in Upper Lake Zurich compared to Sihlsee. Similarly, phosphate concentrations increase during winter (November–April) by ~2–6 μg P L^{-1}. For present PS, these effects are much smaller, as the PS pumping flow is only 5% of that in the extended PS. The prolonged stratification in the reference scenario QNat allows more time for the accumulation of nutrients in the hypolimnion from mineralization at the sediment surface. Until late October, nutrient concentrations are increased by up to ~80 μg N L^{-1} and ~7 μg P L^{-1} for the sum of nitrate and nitrite and phosphate, respectively, compared to the present PS scenario. Seasonal mixing propagates the effects on nutrient concentrations from the hypo- to the epilimnion. Thus, concentrations are raised in the reference scenario QNat from April to December by up to 2.3 μg P L^{-1} and 21 μg N L^{-1} for phosphate and the sum of nitrate and nitrite, respectively.

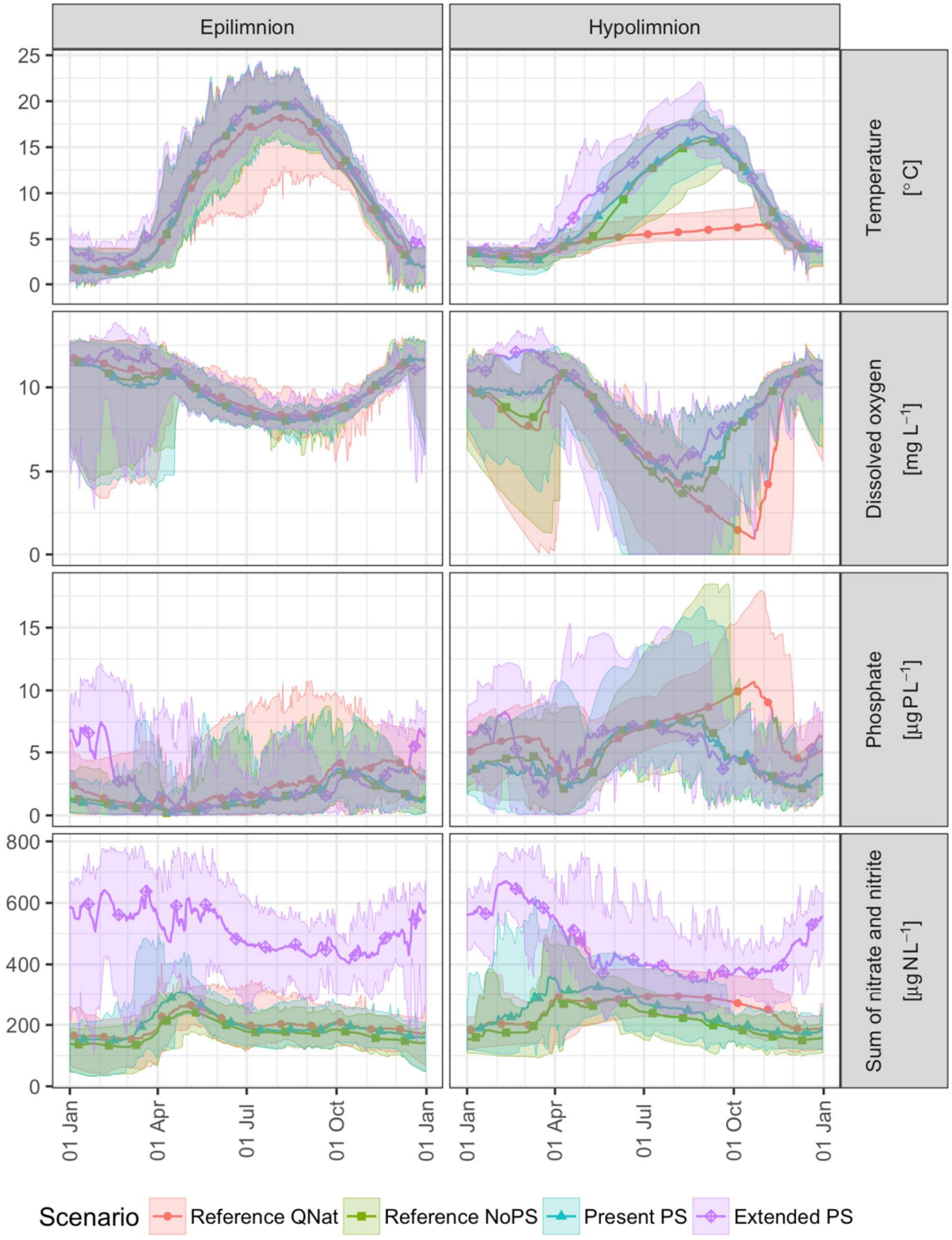

Figure 2. Mean (lines with markers) and range of minima and maxima (shaded areas) of simulated temperatures (°C) and concentrations of dissolved oxygen (mg L^{-1}), phosphate (µg P L^{-1}) and the sum of nitrate and nitrite (µg N L^{-1}) for the two reference scenarios QNat (red) and NoPS (olive-green), the present (turquoise) and the extended PS (violet) scenarios in the epilimnion (uppermost 5 m of the water column) and the hypolimnion (lowermost 5 m of the water column) of Sihlsee.

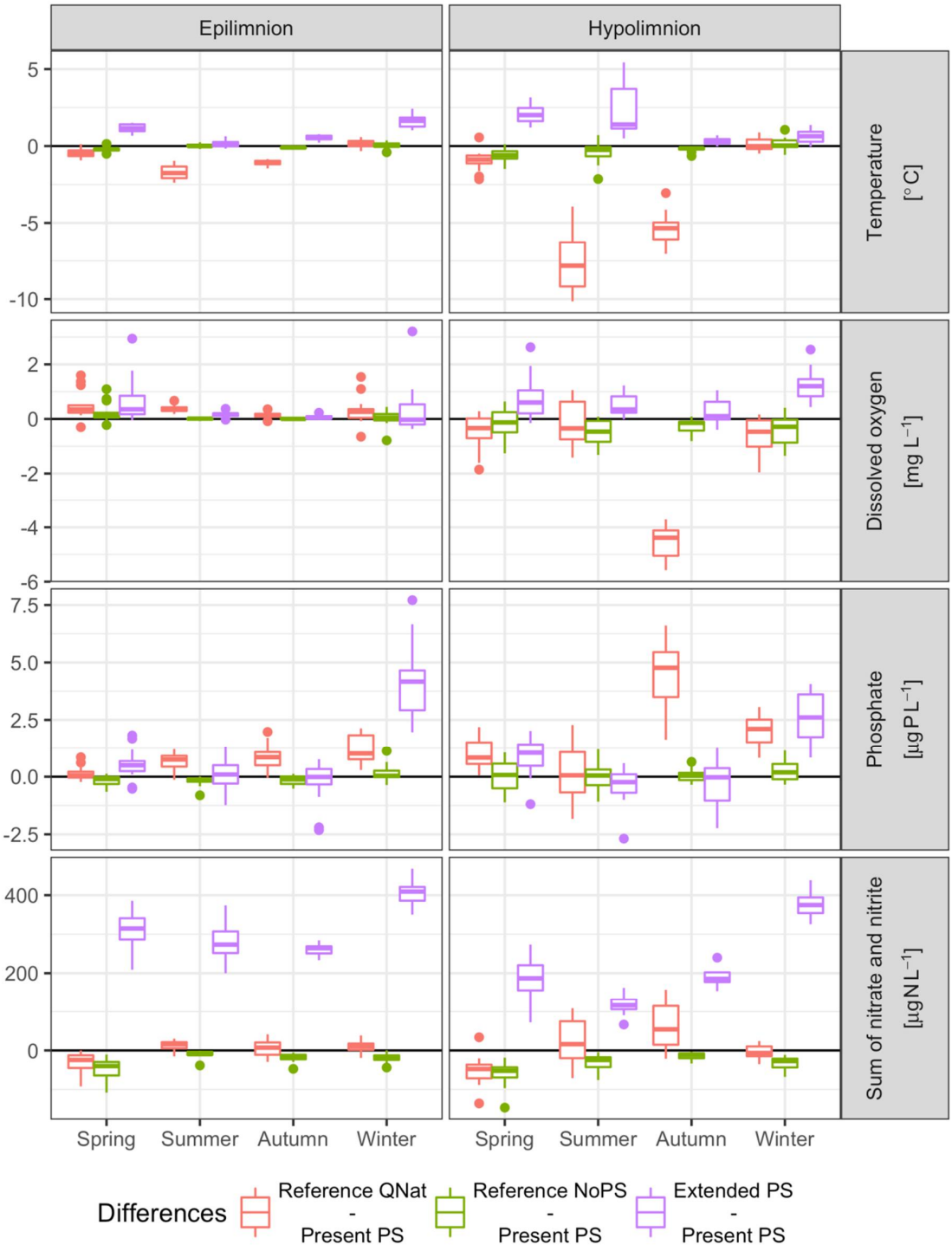

Figure 3. Boxplot of differences in either one of the two reference scenarios NoPS and QNat or the extended PS scenario to the present PS scenario of temperature (°C) and concentrations of dissolved oxygen (mg L^{-1}), phosphate (µg P L^{-1}) and the sum of nitrate and nitrite (µg N L^{-1}) at Sihlsee. Points show outliers; values were aggregated seasonally for each year before plotting (winter: December–February; spring: March–May; summer: June–August; and autumn: September–November).

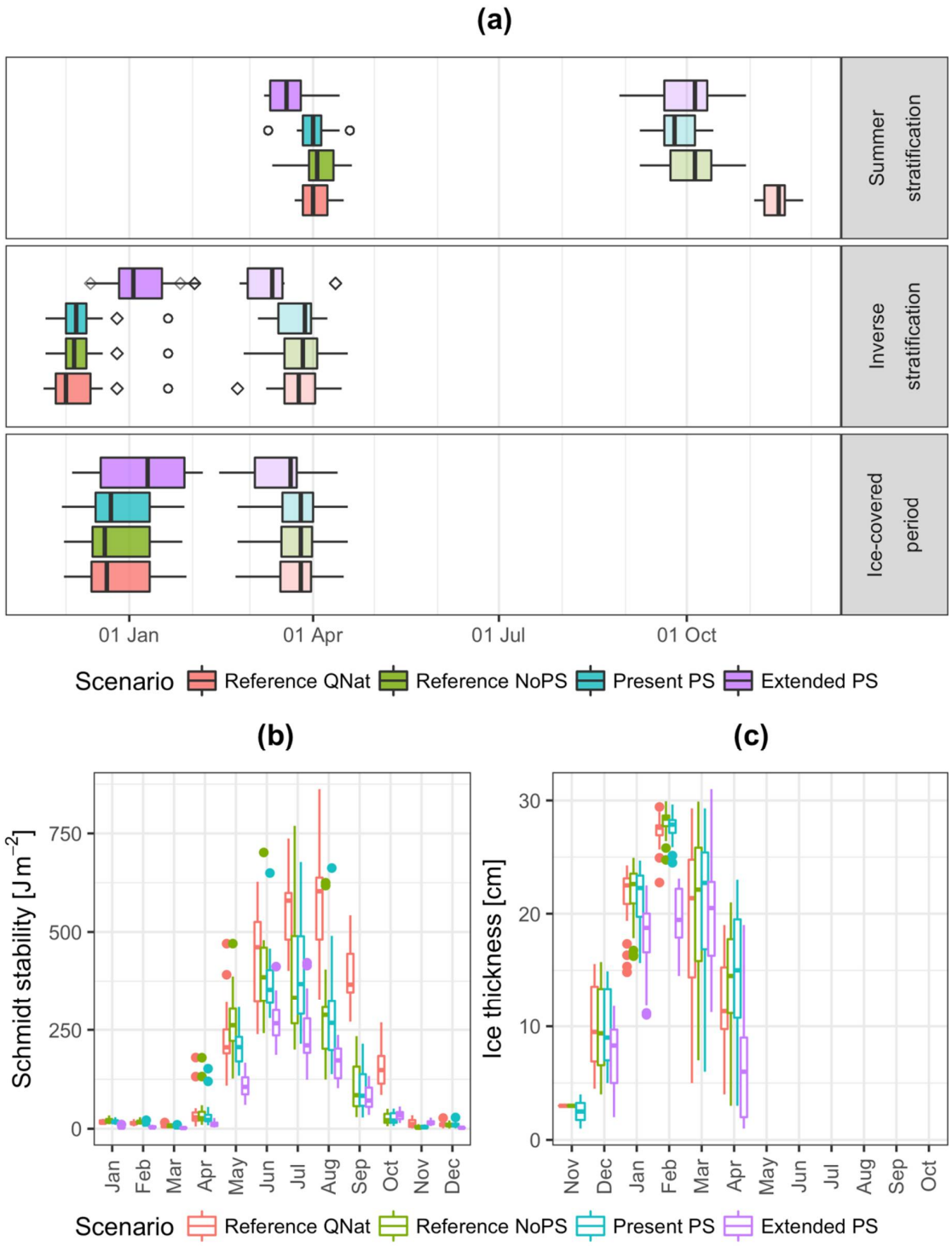

Figure 4. Boxplots for the two reference scenario NoPS and QNat, the present PS and the extended PS scenario at Sihlsee: (**a**) start and end of summer or inverse stratification as well as ice-on and ice-off; (**b**) monthly mean of Schmidt stability (J m^{-2}); and (**c**) monthly mean of ice thickness (cm). Points show outliers of start (circles) and end (squares) of summer or inverse stratification as well as ice-covered period.

5. Discussion

At Sihlsee, extended PS operation is projected to result, compared to the present PS, in: (a) an increase of hypolimnion temperature by ~2 °C during summer due to pumping surface water from

Upper Lake Zurich; (b) warming of surface water by ~1.6 °C during winter and spring mostly due to enhanced mixing; (c) later development of inverse stratification by ~1.5 month; (d) a delay of overturn in spring by ~2 weeks; (e) earlier ice-off by ~1 month and ~30% thinner ice; (f) increased dissolved oxygen concentrations in the hypolimnion; and (g) increased nutrient concentrations originating from higher concentrations in the lower lake. The sum of nitrate and nitrite concentrations in winter and spring are decreasing at Upper Lake Zurich for the same reasons as they increase in Sihlsee. However, effects on Upper Lake Zurich are much less pronounced due to its larger volume and higher natural discharges. Local effects of PS operation in the vicinity of the intake/outlet of the PS hydropower plant are expected to be higher, but their analysis would require 3D simulations in the near field [32].

Besides these effects of PS operations, the simulations highlighted the importance of the withdrawal depth in Sihlsee. If located in the hypolimnion (reference scenario NoPS), the differences to the present PS scenario are minor. Conversely, large effects result if the outlet is placed within the epilimnion (reference scenario QNat) with: (a) hypolimnion temperatures decreasing to commonly observed values of natural lakes in that region; (b) a consequent reduction of epilimnion temperature; (c) delayed summer stratification by ~1.5 months; (d) therefore, reduced dissolved oxygen concentrations; (e) increased phosphate concentrations; and (f) higher sum of nitrate and nitrite concentrations due to delayed seasonal mixing.

These findings can be put into the context of previous modeling studies on pumped-storage hydropower facilities. Additional information about the systems investigated in these studies is given in Supplementary Material S1 (Section D).

Bonalumi et al. [23] showed that both water bodies connected by a PS scheme would mostly be warmed. In autumn, 50% of this warming in the upper hypolimnion of the lower lake would be due to frictional warming of the PS flows. This effect is not as relevant for the case of Sihlsee and Upper Lake Zurich due to the much smaller head. In Lake Oconee, the water column was completely mixed in summer after the introduction of PS operation, whereas before temperature differences between epi- and hypolimnion had ranged between 5 and 13 °C [33]. This is comparable to the strong reduction of Schmidt stability in Sihlsee in the extended PS scenario, but the extent of PS operations is insufficient to completely homogenize it. At Twin Lakes, the PS operation reduced the residence time from 314 to 176 days, resulted in cooling of both basins of Twin Lakes, and weakened stratification [34]. Anderson [18] concluded that the timing of stratification at Lake Elsinore would not be affected by PS, although stratification, expressed as the temperature difference between surface and bottom waters, would be weakened by 1.2 °C in late May. Our findings confirm that summer stratification can be weakened by PS operation. Our results also suggest, in contrast to Anderson [18] and Bermúdez et al. [19], that the timing of stratification can be affected by PS, particularly that of inverse stratification. Regarding the PS impact on temperature, our results indicate a warming of the hypolimnion, which is contrary to the findings of USBR [34], but similar to those of Bonalumi et al. [23] and Potter et al. [33].

Overall, the results of our study showed that the effects of the water exchange due to PS operations, even for extended PS, are small compared to those caused by deep water withdrawal. Similarly, for the drinking water reservoir Grosse Dhuenn [15], selective withdrawal was shown to move the thermocline upwards, increase differences between water temperature of the epi- and hypolimnion, and thus strengthen thermal stratification, when being compared to bottom water withdrawal. These observations highlight the importance of withdrawal depth as a crucial parameter in the design of PS hydropower plants for reducing ecological impacts. However, water temperature and stratification are not the only parameters to be considered for optimizing withdrawal depth, e.g., concentrations of glacial particles might necessitate an intake/outlet placement in the hypolimnion [23].

In the simulations of Bonalumi et al. [23], PS operations were projected to significantly reduce ice cover duration. However, due to a lack of observational data for calibrating the model, this effect could not be reliably quantified. With a modified parameterization of CE-QUAL-W2, we were able

to reliably reproduce ice cover duration (Figure B4 of Supplementary Material S1). With this model, we could show that extended PS would strongly reduce ice thickness and ice-cover duration in Sihlsee.

Water quality parameters, such as dissolved oxygen, and nutrient concentrations, are affected by PS operations through two different mechanisms: exchange of water masses, and indirect effects due to changes in mixing and stratification. The importance of the first mechanism scales with the ratio of the exchanged water masses and the volumes of the basins as shown for example for the sum of nitrate and nitrite in Sihlsee above. Similarly, Bonalumi et al. [23] found inorganic suspended solid concentrations to decrease in the upper reservoir and to increase in the lower lake. At Twin Lakes, inorganic suspended solid concentrations decreased by 40 mg L^{-1} when PS operations were introduced, which was also linked to dilution [34].

Changes in thermal stratification affect water quality in various ways. At Sihlsee, the bottom water withdrawal leads to weaker stratification, and reduces its duration by >1 month. This further affects hypolimnetic dissolved oxygen concentrations: due to less time being available to reduce dissolved oxygen to low levels, more dissolved oxygen being resupplied by mixing through the weaker thermocline, and additional supply of dissolved oxygen as river inflows plunge more easily through a weaker density gradient. Consequently, dissolved oxygen concentrations fall below the legal target of 4 mg L^{-1} in a much smaller volume and during a shorter period. This is in line with the findings of Weber et al. [15] and Anderson et al. [35] that the hypolimnion of a reservoir is more oxygenated when water is withdrawn at the bottom. Likewise, at Twin Lakes, the PS operation seems to have resulted in slight aeration of the hypolimnion, which was considered beneficial, as it increased habitat volume of fish [34].

According to Anderson et al. [35], phosphorus concentrations decrease when water is withdrawn from the hypolimnion. This is in accordance with our findings, as we found additional accumulation in autumn induced by intensified stratification for the reference scenario QNat. Nevertheless, PS impacts on nutrient concentrations are site-specific.

Our projections for effects of PS and deep water withdrawal on temperature and stratification are robust, since they are large compared to the uncertainty of the model, and supported by an extensive data set of temperature for model calibration. The required correction of the water balance and the lack of information to divide the outflow into surface outflow and deep water withdrawal, in the case of flood events, might somewhat affect mixing patterns for these flood events, but should not change the overall picture. The projected effects on water quality include a higher uncertainty, which is due to limited availability of hydrological and water quality forcing of inflows. Nevertheless, the projected changes in water quality yield a coherent picture of the effects of water exchange and those due to changes in thermal stratification.

When recommissioning a PS hydropower plant, a reference state needs to be defined for the environmental impact assessment. For natural lakes, this is the scenario which does not include any artificial PS flows. However, for reservoirs such as Sihlsee, this scenario is mostly a matter of definition: it might be described as the natural state without a lake, where the original river stretch needs to be analyzed; it might also be an artificial state, with the reservoir remaining due to its multiple other purposes, but PS operations being removed. The simulated effects for the reference scenarios NoPS and QNat highlight that the estimated environmental impacts can depend heavily on the choice of the reference scenario. Thus, we see a need for guidelines to define such reference scenarios in the context of assessing environmental impacts of increased development or the extension of PS hydropower plants.

6. Conclusions

Previous studies have shown, by both pre- and post-operational observations and modeling, that PS operations can have significant impacts on temperature and thermal stratification in the connected water bodies. With the present study, we aimed at extending this assessment to indicators of water quality (oxygen and nutrient concentrations) as well as the duration and extent of ice cover.

For this purpose, we projected the effects of a PS extension scenario for the case of Etzelwerk, using a directly coupled hydrodynamic and water quality model for the two connected water bodies. The results showed that PS extension would increase water temperatures in the hypolimnion of the upper reservoir by ~2 °C in summer. The model also projected a significant reduction of the duration and thickness of ice cover due to the PS operations. Additionally, the increased PS pumping flow would raise the nutrient concentrations in the upper reservoir and increase dissolved oxygen availability in its hypolimnion. These effects of PS operation on lake water quality are not easily transferable to other systems, as they depend on the natural, site-specific water quality. In tendency, however, PS supports a decrease of the strength and duration of stratification with correlated effects on dissolved oxygen and nutrients.

Furthermore, we aimed at disentangling the effects of PS operation and deep water withdrawal, which has up to now not been quantified in the context of PS operations. This was achieved by analyzing two reference scenarios: (i) a scenario without hydropower but with deep water withdrawal from the upper reservoir; and (ii) a "quasi-natural" scenario with surface outflow. The scenario without hydropower showed comparably minor differences to the present PS operation. Conversely, the "quasi-natural" scenario highlighted a large effect of the withdrawal depth on the upper reservoir. Compared to the present state, the surface outflow decreased hypolimnetic water temperature by up to ~10 °C, and, accordingly, intensified stratification, and reduced dissolved oxygen concentrations. Thus, we can claim that at Etzelwerk the impacts of water withdrawal in the hypolimnion are more crucial than those of PS operations, especially for the present, but also for the extended PS operation. This also underlines the importance of the location of the PS intake/outlet. Consequently, withdrawal depth in the reference state defines relevant implications for the estimated environmental impacts of a PS scheme. For management purposes, it is, therefore, important to have clear guidelines for defining a reference state as a base scenario for assessing the environmental impacts of increased development or extension of PS hydropower plants. We, thus, recommend for future projects to separately analyze effects due to withdrawal depth and those due to PS operation. Although the effects on the natural lake were small in the present study, these need to be cautiously investigated at any other site.

Supplementary Materials: The following are available online at http://www.mdpi.com/2071-1050/10/6/1968/s1. File S1: "Effects of lake–reservoir pumped-storage operations on temperature and water quality".

Author Contributions: Conceptualization, U.G.K., M.S., and A.W.; Methodology, U.G.K. and M.S.; Software, U.G.K.; Validation, U.G.K. and M.S.; Formal Analysis, U.G.K. and M.S.; Investigation, U.G.K.; Data Curation, U.G.K.; Writing—Original Draft Preparation, U.G.K.; Writing—Review and Editing, M.S. and A.W.; Visualization, U.G.K.; Supervision, M.S., and A.W.; Project Administration, M.S.; and Funding Acquisition, M.S.

Acknowledgments: We want to thank P. Meier for his insights, and M. Schurter, M. Plüss, P. Kathriner and the employees at Etzelwerk for the assistance with fieldwork and lab analysis. We additionally thank MeteoSwiss, FOEN, the Cantonal Environmental Agencies of Schwyz and St. Gallen, WVZ, WSL and Limnex AG for their cooperation and data supply. Funding was provided by the Swiss Federal Railways (SBB AG).

Conflicts of Interest: The authors declare no conflict of interest.

References

1. Barbour, E.; Grant Wilson, I.A.; Radcliffe, J.; Ding, Y.; Li, Y. A review of pumped hydro energy storage development in significant international electricity markets. *Renew. Sustain. Energy Rev.* **2016**, *61*, 421–432. [CrossRef]
2. EU Commission. *Energy Roadmap 2050*; COM(2011) 885; EU Commission: Brussels, Belgium, 2011.
3. REN21. *Renewables 2017 Global Status Report*; REN21 Secretariat: Paris, France, 2017.
4. Evans, A.; Strezov, V.; Evans, T.J. Assessment of utility energy storage options for increased renewable energy penetration. *Renew. Sustain. Energy Rev.* **2012**, *16*, 4141–4147. [CrossRef]
5. Ibrahim, H.; Ilinca, A.; Perron, J. Energy storage systems—Characteristics and comparisons. *Renew. Sustain. Energy Rev.* **2008**, *12*, 1221–1250. [CrossRef]
6. Rehman, S.; Al-Hadhrami, L.M.; Alam, M.M. Pumped hydro energy storage system: A technological review. *Renew. Sustain. Energy Rev.* **2015**, *44*, 586–598. [CrossRef]

7. Deane, J.P.; Gallachòir, B.Ò.; McKeogh, E. Techno-economic review of existing and new pumped hydro energy storage plant. *Renew. Sustain. Energy Rev.* **2010**, *14*, 1293–1302. [CrossRef]
8. Bonalumi, M.; Anselmetti, F.S.; Kägi, R.; Wüest, A. Particle dynamics in high-Alpine proglacial reservoirs modified by pumped-storage operation. *Water Resour. Res.* **2011**, *47*, W09523. [CrossRef]
9. Anderson, M.A. *Technical Analysis of the Potential Water Quality Impacts of LEAPS on Lake Elsinore*; Department of Environmental Sciences, University of California Riverside: Riverside, CA, USA, 2006.
10. Liu, L.X.; Wu, J.C. Research on ice formation during winter operation for a pumped storage station. In *Ice in Surface Waters*; Shen, H.T., Ed.; A. A. Balkema: Rotterdam, The Netherlands, 1999; pp. 753–759.
11. Solvang, E.; Harby, A.; Killingtveit, Å. *Increasing Balance Power Capacity in Norwegian Hydroelectric Power Stations*; SINTEF Energy Report TR A7126; SINTEF Energi: Trondheim, Norway, 2012.
12. Bell, E.; Kramer, S.; Zajanc, D.; Aspittle, J. Salmonid fry stranding mortality associated with daily water level fluctuations in Trail Bridge Reservoir, Oregon. *N. Am. J. Fish. Manag.* **2008**, *28*, 1515–1528. [CrossRef]
13. Hauck, F.R.; Edson, Q.A. Pumped storage: Its significance as an energy source and some biological ramifications. *Trans. Am. Fish. Soc.* **1976**, *105*, 158–164. [CrossRef]
14. Harby, A.; Sauterleute, J.; Korpås, M.; Killingtveit, Å.; Solvang, E.; Nielsen, T. Pumped Storage Hydropower. In *Transition to Renewable Energy Systems*; Stolten, D., Scherer, V., Eds.; Wiley-VCH Verlag GmbH & Co. KGaA: Weinheim, Germany, 2013; pp. 597–618.
15. Weber, M.; Rinke, K.; Hipsey, M.R.; Boehrer, B. Optimizing withdrawal from drinking water reservoirs to reduce downstream temperature pollution and reservoir hypoxia. *J. Environ. Manag.* **2017**, *197*, 96–105. [CrossRef] [PubMed]
16. Romero, J.R.; Antenucci, J.P.; Imberger, J. One- and three-dimensional biogeochemical simulations of two differing reservoirs. *Ecol. Model.* **2004**, *174*, 143–160. [CrossRef]
17. Gebre, S.; Boissy, T.; Alfredsen, K. Sensitivity to climate change of the thermal structure and ice cover regime of three hydropower reservoirs. *J. Hydrol.* **2014**, *510*, 208–227. [CrossRef]
18. Anderson, M.A. Influence of pumped-storage hydroelectric plant operation on a shallow polymictic lake: Predictions from 3-D hydrodynamic modeling. *Lake Reserv. Manag.* **2010**, *26*, 1–13. [CrossRef]
19. Bermúdez, M.; Cea, L.; Puertas, J.; Rodríguez, N.; Baztán, J. Numerical Modeling of the Impact of a Pumped-Storage Hydroelectric Power Plant on the Reservoirs' Thermal Stratification Structure: A Case Study in NW Spain. *Environ. Model. Assess.* **2018**, *23*, 71–85. [CrossRef]
20. Van der Linden, L.; Daly, R.I.; Burch, M.D. Suitability of a Coupled Hydrodynamic Water Quality Model to Predict Changes in Water Quality from Altered Meteorological Boundary Conditions. *Water* **2015**, *7*, 348–361. [CrossRef]
21. Kuo, J.-T.; Lung, W.-S.; Yang, C.-P.; Liu, W.-C.; Yang, M.-D.; Tang, T.-S. Eutrophication modelling of reservoirs in Taiwan. *Environ. Model. Softw.* **2006**, *21*, 829–844. [CrossRef]
22. Liu, W.-C.; Chen, W.-B.; Kimura, N. Impact of phosphorus load reduction on water quality in a stratified reservoir-eutrophication modeling study. *Environ. Monit. Assess.* **2009**, *159*, 393–406. [CrossRef] [PubMed]
23. Bonalumi, M.; Anselmetti, F.S.; Wüest, A.; Schmid, M. Modeling of temperature and turbidity in a natural lake and a reservoir connected by pumped-storage operations. *Water Resour. Res.* **2012**, *48*, WR01184. [CrossRef]
24. Hirsch, P.E.; Eloranta, A.P.; Amundsen, P.-A.; Brabrand, Å.; Charmasson, J.; Helland, I.P.; Power, M.; Sánchez-Hernández, J.; Sandlund, O.T.; Sauterleute, J.F.; et al. Effects of water level regulation in alpine hydropower reservoirs: An ecosystem perspective with a special emphasis on fish. *Hydrobiologia* **2017**, *794*, 287–301. [CrossRef]
25. Bellmore, R.J.; Duda, J.J.; Craig, L.S.; Greene, S.L.; Torgersen, C.E.; Collins, M.J.; Vittum, K. Status and trends of dam removal research in the United States. *Wiley Interdiscip. Rev. Water* **2017**, *4*, e1164. [CrossRef]
26. Cole, T.M.; Wells, S.A. *CE-QUAL-W2: A Two-Dimensional, Laterally Averaged, Hydrodynamic and Water Quality Model, Version 3.71. User Manual*; Department of Civil and Environmental Engineering, Portland State University: Portland, OR, USA, 2013.
27. Bruce, L.C.; Frassl, M.A.; Arhonditsis, G.B.; Gal, G.; Hamilton, D.P.; Hanson, P.C.; Hetherington, A.L.; Melack, J.M.; Read, J.S.; Rinke, K.; et al. A multi-lake comparative analysis of the General Lake Model (GLM): Stress-testing across a global observatory network. *Environ. Model. Softw.* **2018**, *102*, 274–291. [CrossRef]

28. Deliman, P.N.; Gerald, J.A. Application of the Two-Dimensional Hydrothermal and Water Quality Model, CE-QUAL-W2, to the Chesapeake Bay—Conowingo Reservoir. *Lake Reserv. Manag.* **2002**, *18*, 10–19. [CrossRef]
29. Smith, E.A.; Kiesling, R.L.; Galloway, J.M.; Ziegeweid, J.R. *Water Quality and Algal Community Dynamics of Three Deepwater Lakes in Minnesota Utilizing CE-QUAL-W2 Models*; Scientific Investigations Report 2014-5066; US Geological Survey: Reston, VA, USA, 2014; p. 73.
30. Idso, S.B. On the concept of lake stability. *Limnol. Oceanogr.* **1973**, *18*, 681–683. [CrossRef]
31. Der Schweizerische Bundesrat. *Gewässerschutzverordnung vom 28. Oktober 1998 (GSchV)*; SR 814.201; Der Schweizerische Bundesrat: Bern, Switzerland, 1998.
32. Müller, M.; De Cesare, G.; Schleiss, A.J. Flow field in a reservoir subject to pumped-storage operation—In situ measurement and numerical modeling. *J. Appl. Water Eng. Res.* **2018**, *6*, 109–124. [CrossRef]
33. Potter, D.U.; Stevens, M.P.; Meyer, J.L. Changes in physical and chemical variables in a new reservoir due to pumped storage operations. *J. Am. Water Resour. Assoc.* **1982**, *18*, 627–633. [CrossRef]
34. US Bureau of Reclamation (USBR). *Aquatic Ecology Studies of Twin Lakes, Colorado, 1971–1986: Effects of a Pumped-Storage Hydroelectric Project on a Pair of Montane Lakes*; USBR: Denver, CO, USA, 1993.
35. Anderson, M.A.; Komor, A.; Ikehata, K. Flow routing with bottom withdrawal to improve water quality in Walnut Canyon Reservoir, California. *Lake Reserv. Manag.* **2014**, *30*, 131–142. [CrossRef]

Supplementary Material S1 to "Effects of lake-reservoir pumped-storage operations on temperature and water quality"

Ulrike Gabriele Kobler [1,*], Alfred Wüest [1,2] and Martin Schmid [1]

[1] Eawag, Swiss Federal Institute of Aquatic Science and Technology, Surface Waters – Research and Management, CH-6047 Kastanienbaum, Switzerland; ulrike.kobler@eawag.ch, alfred.wueest@eawag.ch, martin.schmid@eawag.ch

[2] EPFL. Physics of Aquatic Systems Laboratory – Margaretha Kamprad Chair, ENAC-IEE-APHYS, CH-1015 Lausanne, Switzerland; alfred.wueest@epfl.ch

* Correspondence: ulrike.kobler@eawag.ch; Tel.: +41 58 765 2210

Sustainability 2018, 10, 1968; doi:10.3390/su10061968 www.mdpi.com/journal/sustainability

A. Model forcing and initial conditions

A.1. Bathymetry

The bathymetry is based on Lidar measurements (terra Vermessungen, October 2014, personal communication) for Sihlsee and on GIS-data of the Federal Institute of Topography (swisstopo Art. 30 GeoIV: 5704 000 000 / DHM25@2003) for Upper Lake Zurich.

Both water basins are divided into 200 m wide segments along the main axis and 0.5-m thick layers (depth). This results in 43 (58) segments and 47 (93) layers for Sihlsee (Upper Lake Zurich). The numbers of segments and layers include at each margin a segment or layer filled with zeros. An overview of the model grid with the positions of all in-, out- and artificial flows is given in Figure A1.

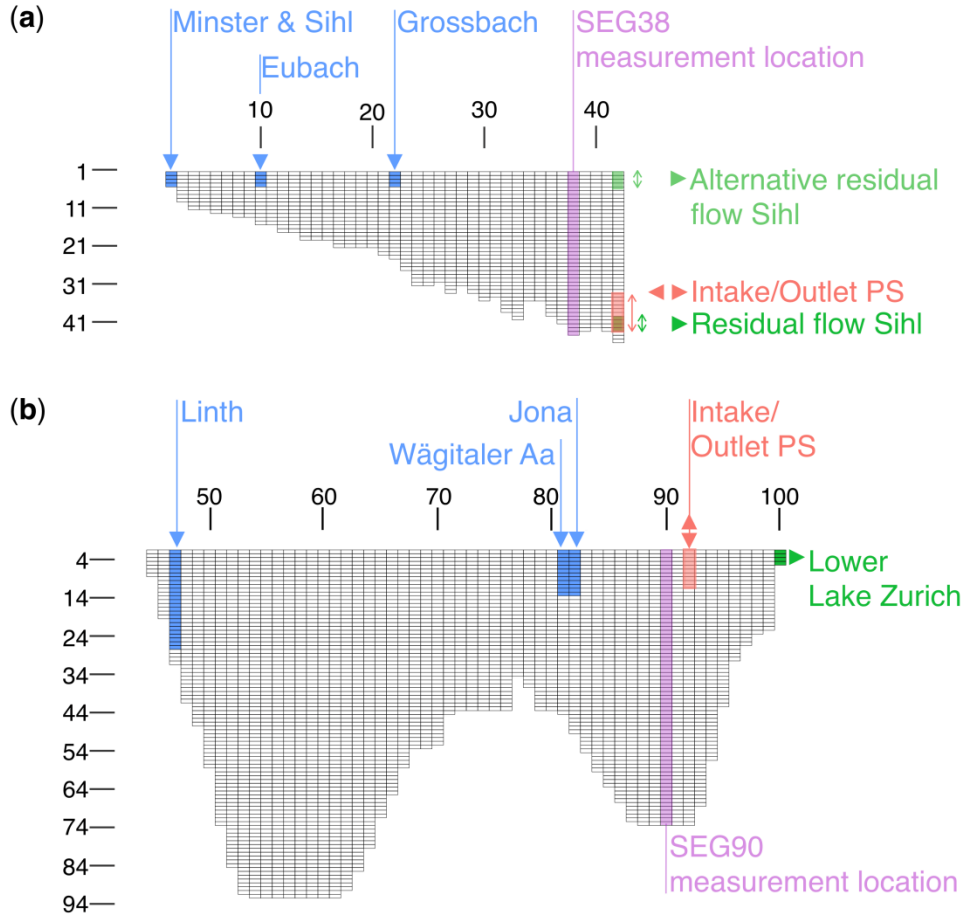

Figure A1. Overview of model grid: Sihlsee (a) and Upper Lake Zurich (b) including the positions of all inflows (blue), outflows (green) and artificial flows (red). The grid labels indicate segment numbers on the horizontal and layer numbers on the vertical axis. The segments with available observations (SEG38 and SEG90) are shaded in violet.

The Sihlsee inflows are located in segments 2 (Minster and Sihl), 10 (Eubach) and 22 (Grossbach), each entering the lake within the top 4 layers. At Upper Lake Zurich the inflows are located in segments 4 (Linth), 37 (Wägitaler Aa) and 38 (Jona). While River Linth is distributed into layers 2-28, the other inflows enter between layers 2-14. The outflow to Lower Lake Zurich is located at segment 58 and implemented as a weir.

The PS intake and outlet of present and extended PS at Sihlsee is located at segment 42 and stretches from layer 33 to 43, that at Upper Lake Zurich is positioned at segment 49 and extends between layers 2 to 12.

The residual flow to River Sihl from Sihlsee is indicated in green in Figure A1. The regular outlet is located at segment 42 between layers 38 to 43, where water is withdrawn for the present PS, the extended PS scenario and the reference scenario NoPS. For the reference scenario QNat the outlet of the residual flow is moved to the surface (weir crest at 887.4 m a.s.l.).

A.2. Meteorological Forcing

For calculating heat exchange at the water surface and mixing processes, the standard version of CE-QUAL-W2 requires the input of air temperature, dew point, wind speed and direction as well as cloudiness and solar radiation. Incoming long-wave radiation is then calculated internally. We replaced this procedure with an external calculation of long-wave radiation and modified the code to read in these values instead of cloudiness, which is then no longer required. Long-wave radiation was calculated according to recommendations given by Flerchinger, *et al.* [1]. Incoming clear-sky long-wave radiation was calculated using the method of Dilley and O'Brien [2]. The cloud correction by Unsworth and Monteith [3], and the elevation correction by Deacon [4] were applied. The albedo of long-wave radiation was kept constant at 0.97.

Table A1. Overview of meteorological information used. Shown are the temporal resolution (h: hourly, d: daily), the time range which was used to generate the meteorological forcing and the order of stations of MeteoSwiss, which were used to fill data gaps: (1) Zurich Fluntern, (2) Wädenswil, (3) Schmerikon and (4) Einsiedeln.

Water body	Variable	Temporal resolution	Time period	Station	Institution	Gap treatment
Upper Lake Zurich	Air temperature	h	01.01.1997-31.12.2015	Wädenswil	MeteoSwiss	(1)
	Dew point	h	01.01.1997-31.12.2015	Wädenswil	MeteoSwiss	(1)
	Wind velocity	h	01.01.1997-31.12.2015	Schmerikon	MeteoSwiss	(2), (1)
	Wind direction	h	01.01.1997-31.12.2015	Schmerikon	MeteoSwiss	(2), (1)
	Cloudiness	d	01.01.1997-31.12.2015	Wädenswil	MeteoSwiss	(1)
	Solar radiation	h	01.01.1997-31.12.2015	Wädenswil	MeteoSwiss	(1)
Sihlsee	Air temperature	h	01.01.1997-31.01.2007	Einsiedeln	MeteoSwiss	(2), (1)
		h	01.02.2007-31.12.2015	Einsiedeln	Segelclub Sihlsee	(4), (2), (1)
	Dew point	h	01.01.1997-31.01.2007	Einsiedeln	MeteoSwiss	(2), (1)
		h	01.02.2007-31.12.2015	Einsiedeln	Segelclub Sihlsee	(4), (2), (1)
	Wind velocity	h	01.01.1997-31.01.2007	Wädenswil	MeteoSwiss	(1)
		h	01.02.2007-31.12.2015	Einsiedeln	Segelclub Sihlsee	(4), (2), (1)
	Wind direction	h	01.01.1997-31.01.2007	Wädenswil	MeteoSwiss	(2), (1)
		h	01.02.2007-31.12.2015	Einsiedeln	Segelclub Sihlsee	(4), (2), (1)
	Cloudiness	d	01.01.1997-29.04.2012	Einsiedeln	MeteoSwiss	(1)
		d	30.04.2012-31.12.2015	Wädenswil	MeteoSwiss	(1)
	Solar radiation	h	01.01.1997-07.03.2012	Wädenswil	MeteoSwiss	(1)
		h	08.03.2012-31.12.2015	Einsiedeln	MeteoSwiss	(2), (1)

The meteorological forcing for Sihlsee was mostly based on observations of MeteoSwiss at Einsiedeln and Segelclub Sihlsee (Figure 1, Table A1). Monitoring of solar radiation and wind speed at an hourly time step at Einsiedeln started only in 2007. For previous years data from the MeteoSwiss station Wädenswil were used. In 2012 the measurement of cloudiness at Einsiedeln was discontinued. Afterwards data were taken from the MeteoSwiss station Zurich Fluntern.

For Upper Lake Zurich, observations of the MeteoSwiss station Wädenswil were used for air temperature, dew point, cloudiness and solar radiation. Wind velocity and direction were taken from the MeteoSwiss station Schmerikon (Figure 1, Table A1). Gaps were filled with data from the closest station (Wädenswil, followed by Zurich Fluntern).

A.3. Hydrological Forcing

For Sihlsee, the discharges of the rivers Minster, Eubach and Grossbach are monitored by the Federal Office for the Environment (FOEN). As inflows of River Sihl and the remaining catchment area were not available, these were estimated by scaling the inflow of Minster proportional to their catchment area. The outflows to River Sihl for present and extended PS are based on simulations of the Swiss Federal Institute for Forest, Snow and Landscape Research [5]. These simulations give the total flow in River Sihl downstream of the dam, composed of the sum of discharges through the regular outlet and those of floods over the spillway. Since all water is withdrawn from the bottom outlet in the model, the simulated flow patterns during flood events may be different to those actually occurring in the reservoir.

The outflow of the two reference scenarios (QNat and NoPS) is based on a modelling study of LIMNEX AG (personal communication). In case of QNat the outflow is implemented using a weir (Figure A1, upper edge at 884.7 m a.s.l., 5 m wide, weir discharge coefficient 0.7) which directly allows the computation of the discharge following the formula of Poleni [6]. For NoPS, the discharge computed with CE-QUAL-W2 for QNat was used, but withdrawn from the hypolimnion instead of being discharged over a weir (Figure A1). Figure A2 depicts the PS flows as well as the residual flow to river Sihl for the reference scenarios QNat and NoPS, the present PS and the extended PS scenarios.

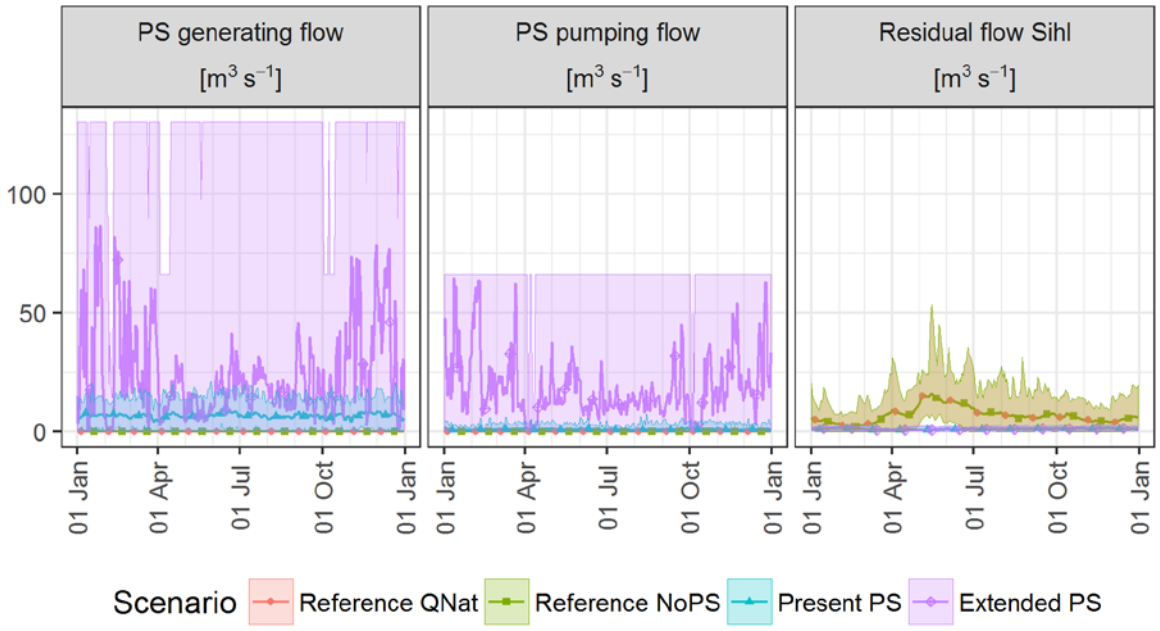

Figure A2. PS generating and PS pumping flow as well as residual flow to river Sihl ($m^3 s^{-1}$) for the reference scenario QNat and NoPS, the present PS and the extended PS scenario. Shown are means (lines with markers) and range of minima and maxima (shaded areas) of simulated years 1998-2012.

To account for measurement errors as well as missing inflows, groundwater exchange, evaporation and precipitation at Sihlsee we estimated a correction term to achieve agreement with observed water levels. Simulated and observed water levels were converted to the corresponding volume for each day, and their difference was averaged for each month. The monthly missing volume was then implemented as a distributed tributary, which could also have negative values.

Of the inflows to Upper Lake Zurich, only the discharge of River Linth at Weesen is routinely monitored by FOEN. As no additional information was available, this discharge was used to scale the other inflows by the corresponding ratio of catchment area. The outflow to Lower Lake Zurich was implemented through a weir (upper edge at 405.5 m a.s.l., 200 m wide, weir discharge coefficient 0.5).

Both scenario-independent and scenario-dependent hydrological forcing of Sihlsee and Upper Lake Zurich are given in Table 1. While no PS flows are withdrawn in case of the reference scenarios (NoPS and QNat), extended PS increases PS generating and PS pumping flows by factors of ~4 and ~22, respectively (Figure A2). Based on the hydrological forcing the average water residence time in Sihlsee can be estimated to 150 days for the reference scenarios, 135 days for present PS and 40 days for extended PS.

The basic dataset of hourly exchange flows for the extended PS scenario was provided by the Swiss Federal Railways and considered monthly-averaged net inflows to Sihlsee. It needed adaptation to allow assessing the influence of floods and low flows. Thus, the PS flows of the extended PS scenario were adapted based on the formulation of an hourly water balance, with hourly natural in- and outflows, where the resulting water level is limited by minimum and maximum operational water levels as well as temporal restrictions for the minimal water level from June to October.

A.4. Inflow Water Quality Forcing

FOEN provides water temperature observations at Rivers Alp and Linth for the considered simulation period (Figure 1). The River Alp was chosen to be representative for all inflows of Sihlsee and the River Linth for those of Upper Lake Zurich. Inflow temperatures for Sihlsee range from ~1 °C in winter to ~18 °C in summer. River Linth is the outflow of Walensee and thus significantly warmer in winter with average temperatures ~6 °C.

Inorganic suspended solid concentrations of the inflows of Sihlsee were estimated based on Keller and Weibel [7]. They derived an empirical relationship between stream flow in mm per week and suspended solid concentrations in mg-L^{-1} for two sub-catchments of River Alp. Out of the two, Erlenbach (referred to as 10 in their publication) was chosen as it corresponds better to the catchment of Sihlsee. Thus, the regression listed on page 57 of their publication was used to estimate inorganic suspended solid concentrations for all inflows of Sihlsee. Inorganic suspended solid concentrations of the inflows of Upper Lake Zurich were estimated as follows: for Linth, Peters-Kümmerly [8] determined a direct relationship between discharge and the load of suspended solids. The estimated regression follows Eq.1.

$$c = 1.15 \cdot Q^{0.04}, \quad (1)$$

with c in mg L^{-1} and Q in m^3 s^{-1}. Additional information for the other inflows to Upper Lake Zurich was missing, thus inorganic suspended solid concentrations were estimated with the same procedure as for Sihlsee. When calibrating the model, inorganic suspended solid concentrations were scaled for both water bodies with the parameter f_{ISS}.

Dissolved oxygen concentrations were estimated according to Haynes [9], assuming equilibrium with the atmosphere, using the water temperature of the inflows. Nutrient concentrations of the sum of nitrate and nitrite, ammonium and phosphate were considered as forcing for all the inflows. For Sihlsee, these were approximated with observations at Erlenbach, a sub-catchment of River Alp (Figure 1). There nitrate, total nitrogen and phosphate have been observed weekly as part of a national monitoring program (NADUF) since 2003. Ammonium, not directly observed, was approximated by the difference of total nitrogen and nitrate. Weekly

averages of all years between 2003-2015 were used to generate a mean annual forcing, which was assigned to the nutrient forcing for all simulated years. During model calibration these time series were scaled with the parameters f_{PO4}, f_{NO} and f_{NH4} (Section B.2). For Upper Lake Zurich, the mean annual nutrient concentrations were calculated based on monthly observations in River Linth (1997-2014). As the observations of the other inflows to Upper Lake Zurich are not as comprehensive, these average annual nutrient concentrations were also assigned to the nutrient forcing of the other inflows. The parameters f_{PO4}, f_{NO} and f_{NH4} (Section B.2) were adjusted during model calibration to scale the water quality time series for Linth and the other two inflows separately, as the concentrations differ substantially according to Gammeter and Forster [10].

A.5. Initial conditions

The initial conditions for both water bodies are given in Table A2. The model was initialized on 01 January. At this time, Upper Lake Zurich is usually homogenized, while Sihlsee is inversely stratified. For Upper Lake Zurich, constant values corresponding to average observed winter conditions or to default values of CE-QUAL-W2 were set as initial conditions. For Sihlsee, an inversely stratified temperature profile was assumed, whereas water quality parameters were set to constant values. The first year of the simulations was excluded from the analysis, and due to the relatively short residence times, the initial conditions have only a minor impact on the simulation results in the subsequent years.

Table A2. Initial conditions of temperature, ice thickness and concentrations of inorganic suspended solids, phosphate, ammonium, sum of nitrate and nitrite, labile dissolved organic matter (LDOM), refractory dissolved organic matter (RDOM), labile particulate organic matter (LPOM), refractory particulate organic matter (RPOM), algal groups 1 and 2, dissolved oxygen and zooplankton. Temperature at Sihlsee was input as profile.

		Sihlsee										Upper Lake Zurich
Variable	**Layer**	**2-46**	**2**	**3**	**4**	**5**	**6**	**7**	**8**	**9**	**10-46**	**2-92**
	Unit											
Temperature	[°C]		0.8	0.9	1	1.5	2	2.5	3	3.5	4	6
Ice thickness	[m]	0.1										0
Inorg. suspended solids	[mg L^{-1}]	2										2
Phosphate	[µg P L^{-1}]	5										5
Ammonium	[µg N L^{-1}]	2										2
Sum of nitrate and nitrite	[µg N L^{-1}]	300										700
LDOM	[mg L^{-1}]	0.1										0.1
RDOM	[mg L^{-1}]	0.1										0.1
LPOM	[mg L^{-1}]	0.1										0.1
RPOM	[mg L^{-1}]	0.1										0.1
Algae group 1	[mg L^{-1}]	0.05										0.05
Algae group 2	[mg L^{-1}]	0.05										0.05
Dissolved oxygen	[mg L^{-1}]	10										11
Zooplankton	[mg L^{-1}]	0.01										0.01

B. Available observations at Sihlsee and Upper Lake Zurich and model calibration

B.1. Available observations

The observations at Sihlsee, were conducted by Eawag solely for the purpose of this study from April 2014 to December 2016. Temperatures, observed quasi-continuously (Figure B1), show that seasonal convective mixing occurred latest in mid-October, and inverse stratification started to evolve at end-December, facilitating ice growth dependent on meteorological conditions. In winter 2014/15 the lake was ice covered, but not in winter 2015/16. Summer stratification arose between beginning and mid-April with maximum temperatures between 20 and 25 °C and 15 to 17 °C in the epi- and hypolimnion, respectively. Summer hypolimnion temperatures are high compared to most stratified Swiss lakes, where they generally remain below 10 °C throughout the year. As shown in the present study, these high hypolimnion temperatures are caused by deep water withdrawal in the lake.

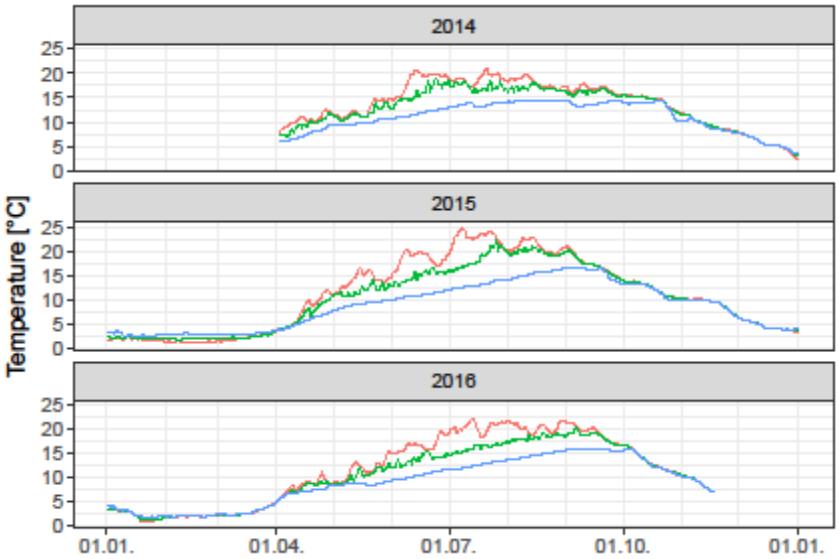

Figure B3. Observed water temperature in Sihlsee for 2014-2016 at three depths: 1 m below surface (red), 6 m below surface (green), 0.5 m above sediment (blue); measurements were performed at SEG38 (Figure 1).

Vertical profiles of additional physical and chemical parameters were measured on a monthly basis from April 2014 to December 2016 (26 profiles for inorganic suspended solids and nitrate, 25 for dissolved oxygen, 16 for Chlorophyll-a, 24 for total phosphorus). Observed inorganic suspended solid concentrations were homogeneously distributed at ~5 mg L^{-1} in April and from October to December. During summer stratification inorganic suspended solid concentrations were ~5 and <30 mg L^{-1} in the epi- and the hypolimnion, respectively. One flood event on 22 July 2014 caused ISS concentration peaks in the thermocline. In August and September, dissolved oxygen concentrations in the hypolimnion fell below 4 mg L^{-1}, the legal requirement in Switzerland [11]. Chlorophyll-a concentrations did not exceed 3.5 µg L^{-1}, with highest values for June, August and September. Observed nitrate concentrations varied between 100 and 350 µg N L^{-1}, with decreased concentrations in the epilimnion due to algal uptake from June to September. Nitrite concentrations were <10 µg N L^{-1} for the 2 observations made. Total phosphorus was <35 µg P L^{-1}, with enriched concentrations in the hypolimnion for July and September and epilimnion concentrations <10 µg P L^{-1} throughout the year. Thus, Sihlsee can be considered oligotrophic.

The observations at Upper Lake Zurich are part of a monitoring program by the cantonal agencies [10,12]. The observed temperature (1994-2005) during summer stratification was 5-6 °C and 20-25 °C for the hypo- and the epilimnion, respectively [10]. From December to April, the lake was mixed and in some winters inversely stratified with a minimum surface temperature of ~2 °C. Wind protected bays can freeze over during very cold winters [10]. No observations are available for inorganic suspended solid concentrations. The hypolimnetic dissolved oxygen concentrations at SEG90 (Figure 1) for 1994-2005 fell below 4 mg L^{-1} every year during the stagnation period. Chlorophyll-a concentrations did not exceed 6 µg L^{-1} for 2006-2010. The mean annual concentrations (1996-2010) of nitrate, nitrite and ammonium were 700, 5 and 10 µg N L^{-1} and those of orthophosphate were ~10 µg P L^{-1}. The annual mean of the total phosphorus concentrations did not exceed 12 µg P L^{-1}. Thus, Upper Lake Zurich can be classified as mesotrophic.

B.2. Model Calibration

The model was calibrated manually with a manual trial and error approach, with the aim of minimizing root mean square errors (RMSE), mean absolute errors (MAE) and mean errors (ME) between simulated and observed quantities. Additionally, the differences between observed profile and time series data and simulations were visually inspected. Several model parameters of

CE-QUAL-W2 and factors for adjusting the water quality forcing (Section A) of both water bodies were calibrated, while the majority of the other parameters was either set to the default value or determined based on literature values [13-15].

RMSEs are given in Table 2 of the main manuscript, MAEs and MEs in Table B1. Moreover, temperature profiles at Sihlsee and Upper Lake Zurich show a good agreement for the calibration period (2014-2015) (Figure B2, Figure B3). Similar to the RMSEs (Table 2) MAEs and MEs shows that dissolved oxygen and nutrient concentrations are better predicted in the epi- than in the hypolimnion.

The comparison of simulated and observed ice-thickness is show in Figure B4, where observations were provided by the Swiss Federal Railways, and volumetrically averaged time series of observed and simulated variables for epi- and hypolimnion are shown in Figure B5 and B6 for Sihlsee and Upper Lake Zurich, respectively. While in the epilimnion concentrations are either overestimated (sum of nitrate and nitrite) or underestimated (total phosphorus), the average in the hypolimnion is reproduced satisfactorily. The model is, however, not capable of reproduction peak concentrations, which typically occur during floods. A list of model parameters with a description, and their corresponding default and calibrated values are given in Table B2.

Table B3. Mean absolute error (MAE) and mean error (ME) of temperature, dissolved oxygen, the sum of nitrate and nitrite as well as total phosphorus computed for the entire water column, the epilimnion and the hypolimnion of Sihlsee or Upper Lake Zurich (na: not available).

Variable	Unit	Sihlsee 2014-2015			Upper Lake Zurich 1998-2015		
		Entire water column	Epi-limnion [1]	Hypo-limnion [2]	Entire water column	Epi-limnion [1]	Hypo-limnion [3]
Mean absolute error (MAE)							
Temperature	[°C]	0.71	0.69	0.75	0.63	0.54	0.65
Dissolved oxygen	[mg L^{-1}]	0.90	0.82	1.05	0.98	0.83	0.93
Inorg. suspended solids	[mg L^{-1}]	2.78	1.13	4.34	na	na	na
Sum of nitrate and nitrite	[µg N L^{-1}]	61	58	69	91	114	91
Total phosphorus	[µg P L^{-1}]	2.86	2.03	4.14	2.95	2.96	2.88
Mean error (ME)							
Temperature	[°C]	0.41	0.58	0.28	-0.11	0.02	-0.23
Dissolved oxygen	[mg L^{-1}]	0.36	-0.10	0.94	0.49	0.00	0.35
Inorg. suspended solids	[mg L^{-1}]	1.55	0.56	1.90	na	na	na
Sum of nitrate and nitrite	[µg N L^{-1}]	21	14	18	16	70	26
Total phosphorus	[µg P L^{-1}]	-1.20	-0.76	-2.64	-1.75	-2.03	-1.76

[1] Uppermost 5 m of the water column. [2] Lowermost 5 m of the water column. [3] All depths ≥ 20 m.

Table B2. Model parameters deviating from the default values of CE-QUAL-W2. Given are the values for both water bodies and the default value of CE-QUAL-W2. The column on the right indicates whether the parameters where selected from literature (in capital letters) or computed by calibration (cal). The capital letters stand for: A: Bonalumi, *et al.* [14], B: Mieleitner and Reichert [13], C: Mieleitner and Reichert [15].

		Sihlsee	Upper Lake Zurich	Default	Based on
Inorganic suspended solids					
SSS	Settling velocity [m d^{-1}]	0.2	0.2	1	
SEDRC	Sediment resuspension	ON	ON	OFF	A
TAUCR	Critical shear stress for sediment resuspension	0.001	0.001	1	
Gas exchange					
EQN#	Equation used to calculate gas exchange	5	5	6	A
Parameters nitrification and denitrification					
NH4T1	Lower temperature for ammonia decay [°C]	0	0	5	cal
NO3T1	Lower temperature for nitrate decay [°C]	0	0	5	

Continuation Table B2.

		Sihlsee	Upper Lake Zurich	Default	Based on
Parameters nitrification and denitrification					
ORGP	Organic matter stoichiometric coefficient for phosphorus [-]	0.0087	0.0087	0.005	B
ORGN	Organic matter stoichiometric coefficient for nitrogen [-]	0.08	0.08	0.08	cal
Parameters organic matter					
OMT1	Lower temperature for organic matter decay [°C]	0	0	4	cal
OMT2	Upper temperature for organic matter decay [°C]	30	30	25	
Parameters sediment					
NH4R	Sediment release rate of ammonium, fraction of SOD-rate	0.02	0.02	0.001	cal
SEDC	Detailed sediment- diagenesis-model	ON	ON	OFF	
SEDCI	Initial sediment concentration [g m^{-2}]	0.01	0.01	0	
SOD	Anaerobic sediment release rate [g m^{-2} d^{-1}]	0.4	1		
DYNSEDK	Dynamic computation first-order-model	ON	ON	OFF	
SODT1	Lower temperature for sediment decay [°C]	0	0	4	
Mixing parameters					
FRIC	Chézy friction coefficient [$m^{0.5}$ s^{-1}]	70	70		A
AX	Longitudinal Eddy-Viscosity [m^2 s^{-1}]	0.1	0.1	1	
DX	Longitudinal Eddy-Diffusivity [m^2 s^{-1}]	0.1	0.1	1	
AZMAX	Maximum vertical Eddy-Viscosity [m^2 s^{-1}]	0.1	0.1	1	
FI	Internal friction [-]	0.01	0.01	0.015	
Scaling of meteorological forcing					
SHD	Shading coefficient [-]	0.85	0.90	1	cal
WSC	Wind sheltering coefficient [-]	1.35	1.25	1	
Scaling of water quality forcing of inflows					
f_{ISS}	Multiplier inorganic suspended solids [-]	0.25	1.00 | 0.25[1]		cal
f_{PO4}	Multiplier phosphate [-]	4.58	1.00 | 32.5[1]		
f_{NH4}	Multiplier ammonium [-]	0.17[2]	0.65 | 0.72[1]		
f_{NO}	Multiplier nitrate + nitrite [-]	1.42	1.10 | 4.86[1]		
Heat exchange at air water interface					
AFW	Coefficient wind function [W m^{-2} mm Hg^{-1}]	5.87	5.87	9.2	A
BFW	Coefficient wind function [W m^{-2} mm Hg^{-1} (m s^{-1})$^{-CFW}$]	2.42	2.42	0.46	
CFW	Coefficient wind function	1	1	2	
Heat exchange at sediment water interface					
TSED	Temperature sediment [°C]	5	7	10	cal
CBHE	Coefficient heat exchange [W m^{-2} $°C^{-1}$]	$1.0x10^{-6}$	$1.0x10^{-6}$	0.3	A
Light attenuation water column					
EXH2O	Attenuation pure water [m^{-1}]	0.2	0.2	0.25	cal
BETA	Fraction incident solar radiation absorbed at water surface [-]	0.35	0.35	0.45	

[1] The two multipliers for inflow water quality at Upper Lake Zurich were used for River Linth and the other two inflows (Jona and Wägitaler Aa), respectively.

[2] As ammonium was not observed, the difference of total nitrogen and nitrate and nitrite was taken as proxy and adapted with the given factor.

Continuation Table B2.

		Sihlsee / Upper Lake Zurich			Based on
		Group 1	**Group 2**	**Default**	
Parameters phytoplankton					
AG	Max. growth rate phytoplankton [d^{-1}]	1.9	1.4	2	cal/C
AR	Max. respiration rate phytoplankton [d^{-1}]	0.05	0.05	0.04	B
AE	Max. excretion rate phytoplankton [d^{-1}]	0.015	0.015	0.04	cal
AM	Max. mortality rate phytoplankton [d^{-1}]	0.015	0.015	0.1	cal
AS	Algal settling rate [m d^{-1}]	0.08	0.01	0.1	C
ALGP	Algal stoichiometric coefficient for phosphorus [-]	0.0087	0.0087	0.005	B
ALGN	Algal stoichiometric coefficient for nitrogen [-]	0.08	0.08	0.08	cal
ALPOM	Fraction of algal biomass converted to POM when dying	0.9	0.9	0.8	B
AHSP	Algal half-saturation for phosphor [g m^{-3}]	0.0007	0.0013	0.003	C
AT1	Lower temperature for algal growth [°C]	0	0	5	cal
AT2	Lower temperature for max. algal growth [°C]	11	11	25	
AT3	Upper temperature for max. algal growth [°C]	15	15	35	
AT4	Upper temperature for algal growth [°C]	30	30	40	
ACHLA	Ratio algal biomass to chlorophyll a [mg Algae (µg Chl a)$^{-1}$]	0.1	0.1	0.05	
Parameters zooplankton					
ZG	Max. growth rate zooplankton [d^{-1}]	0.7		1.5	cal
ZP	Zooplankton stoichiometric coefficient for phosphorus [-]	0.0087		0.005	B
ZN	Zooplankton stoichiometric coefficient for nitrogen [-]	0.08		0.08	cal
ZT1	Lower temperature for zooplankton growth [°C]	0		5	
ZT2	Lower temperature for max. zooplankton growth [°C]	20		25	
ZT3	Upper temperature for max. zooplankton growth [°C]	30		35	
ZT4	Upper temperature for zooplankton growth [°C]	35		40	

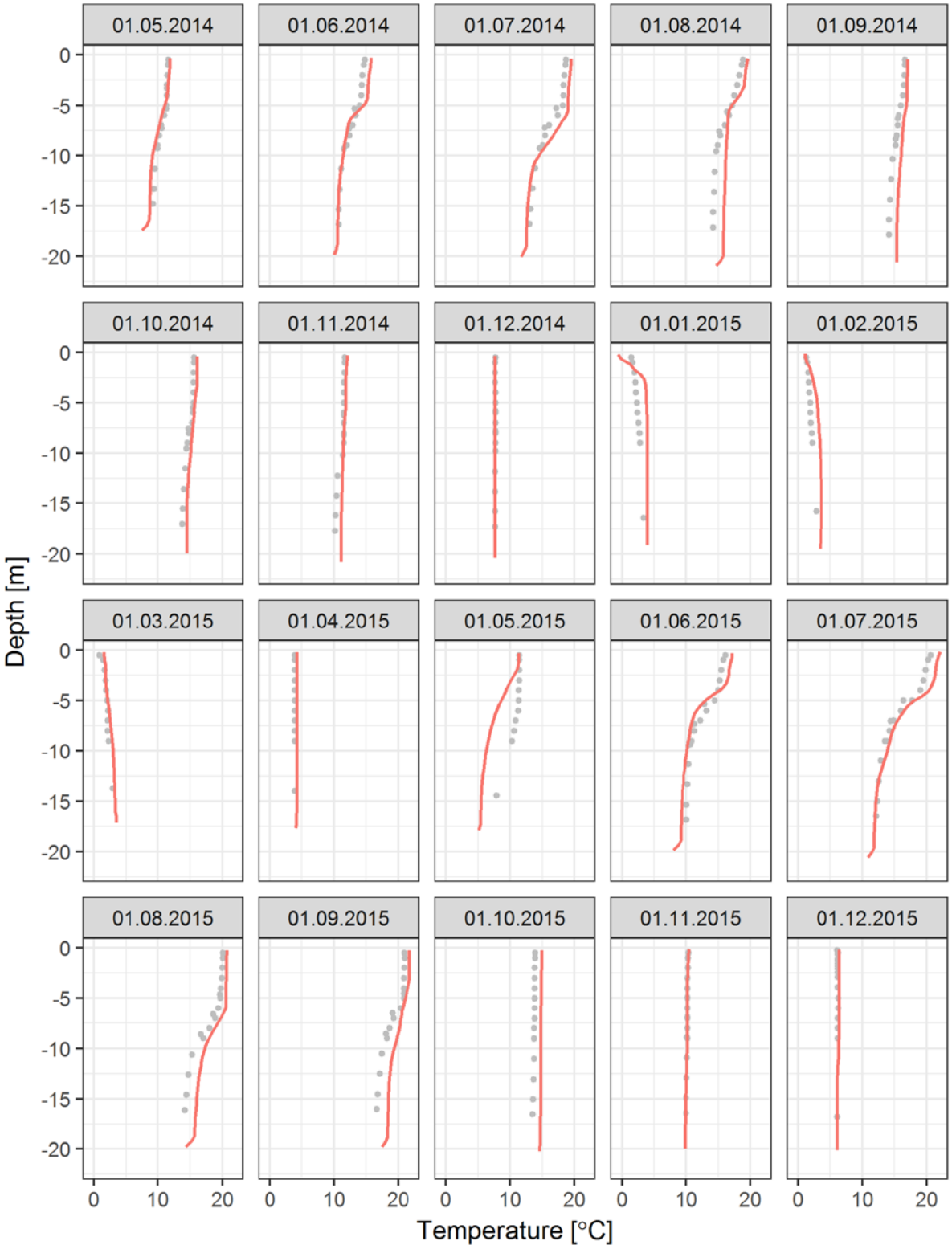

Figure B4. Simulated (red) and observed (grey) temperatures (°C) at Sihlsee.

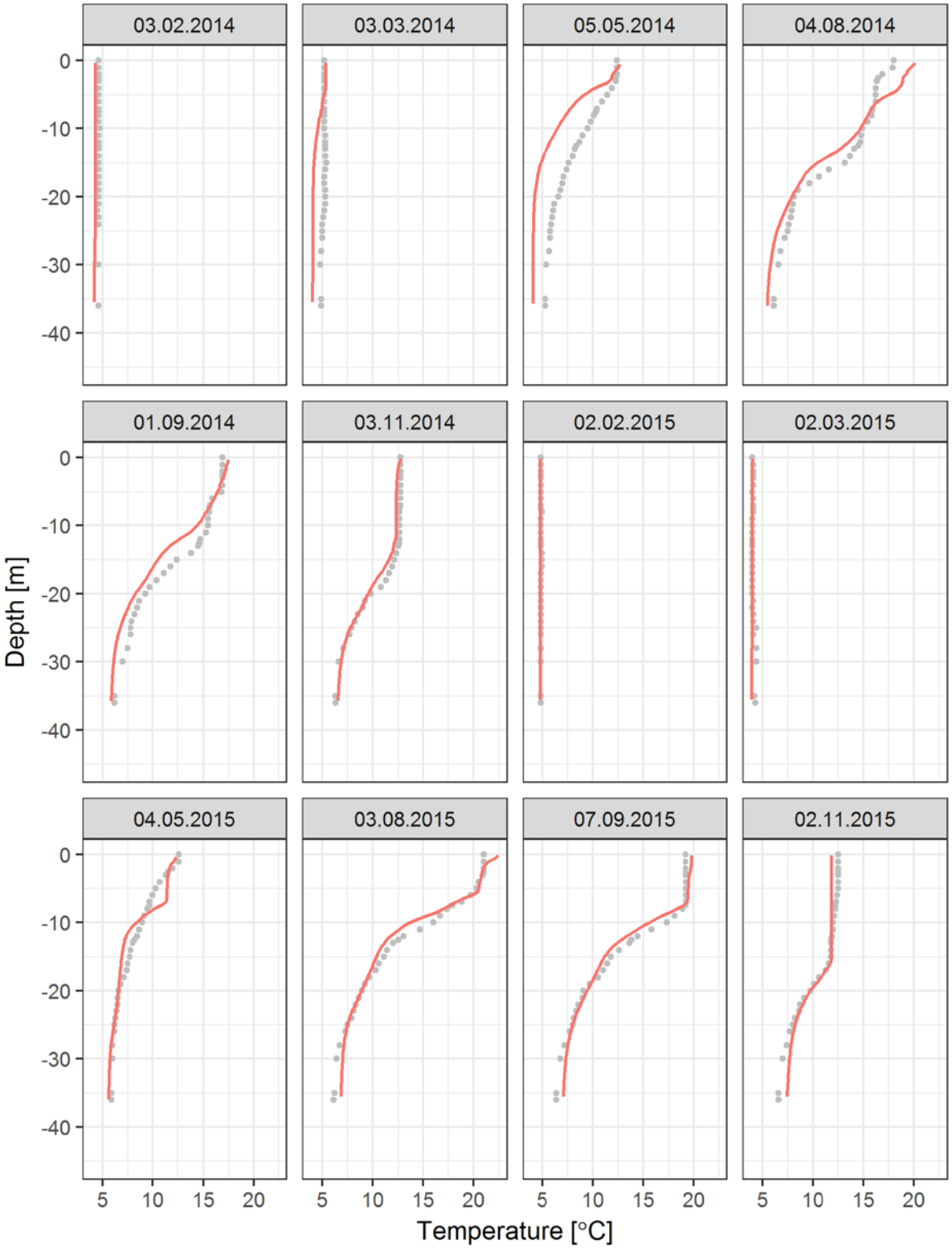

Figure B5. Simulated (red) and observed (grey) temperatures (°C) at Upper Lake Zurich.

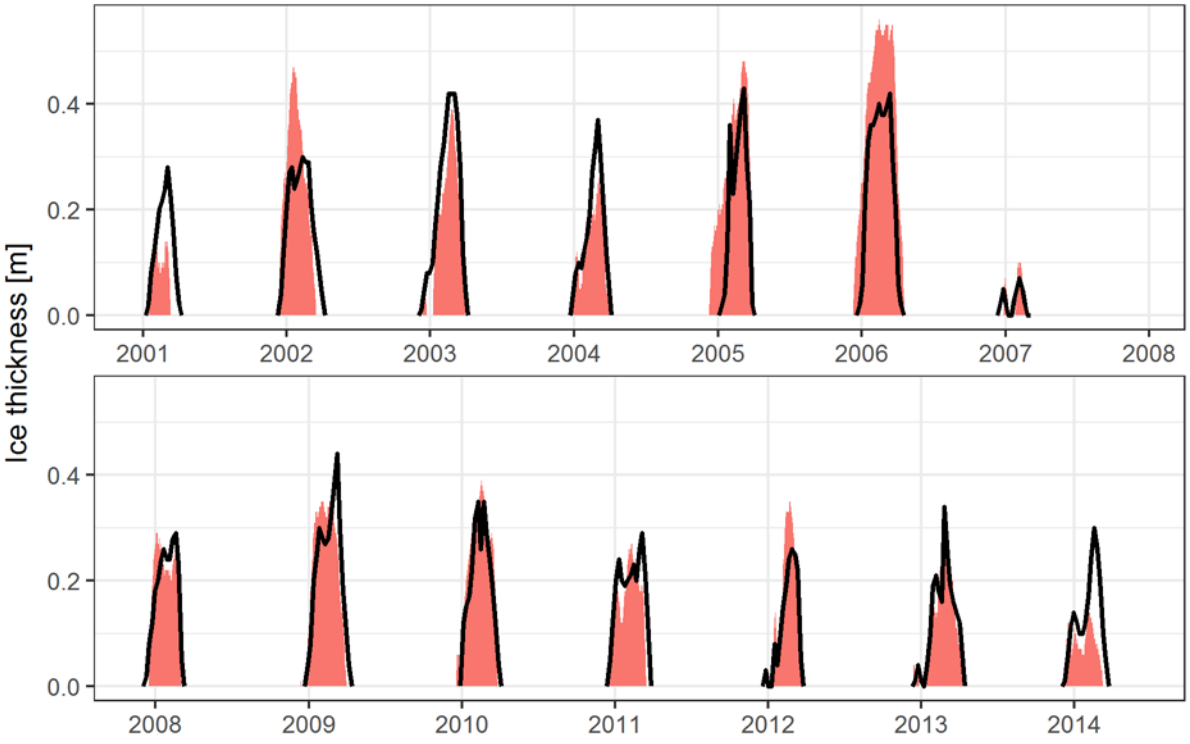

Figure B6. Simulated (red) and observed (black) ice thickness (m) at Sihlsee from 2001-2014.

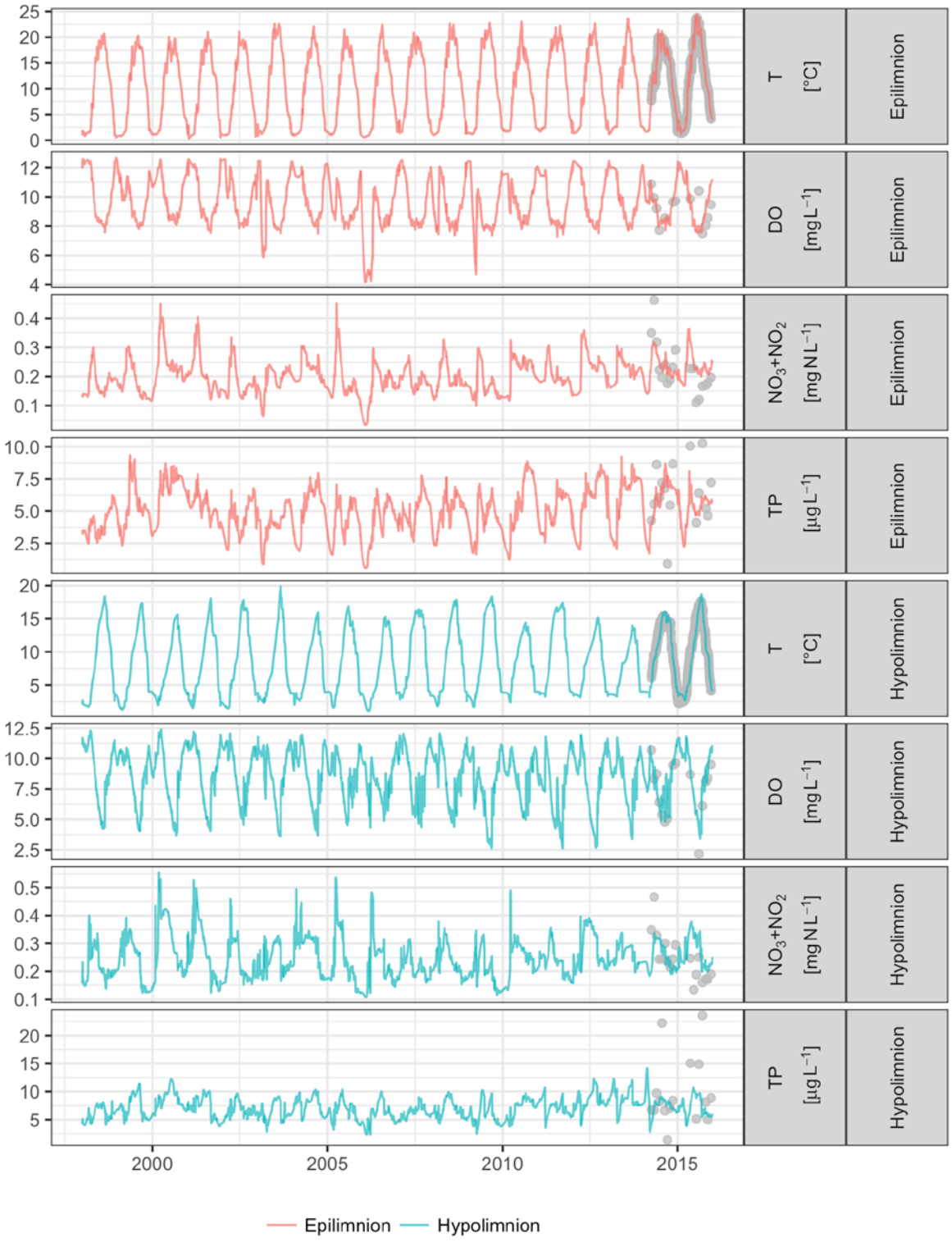

Figure B5. Time series of simulated (lines) and observed (grey points) variables at Sihlsee; depicted are temperature (T) in °C, dissolved oxygen (DO) in mg L^{-1}, sum of nitrate and nitrite (NO_3+NO_2) in µg N L^{-1} and total phosphorus (TP) in µg P L^{-1} all aggregated volumetrically for either epi- (uppermost 5 m of the water column) or hypolimnion (lowermost 5 m of the water column).

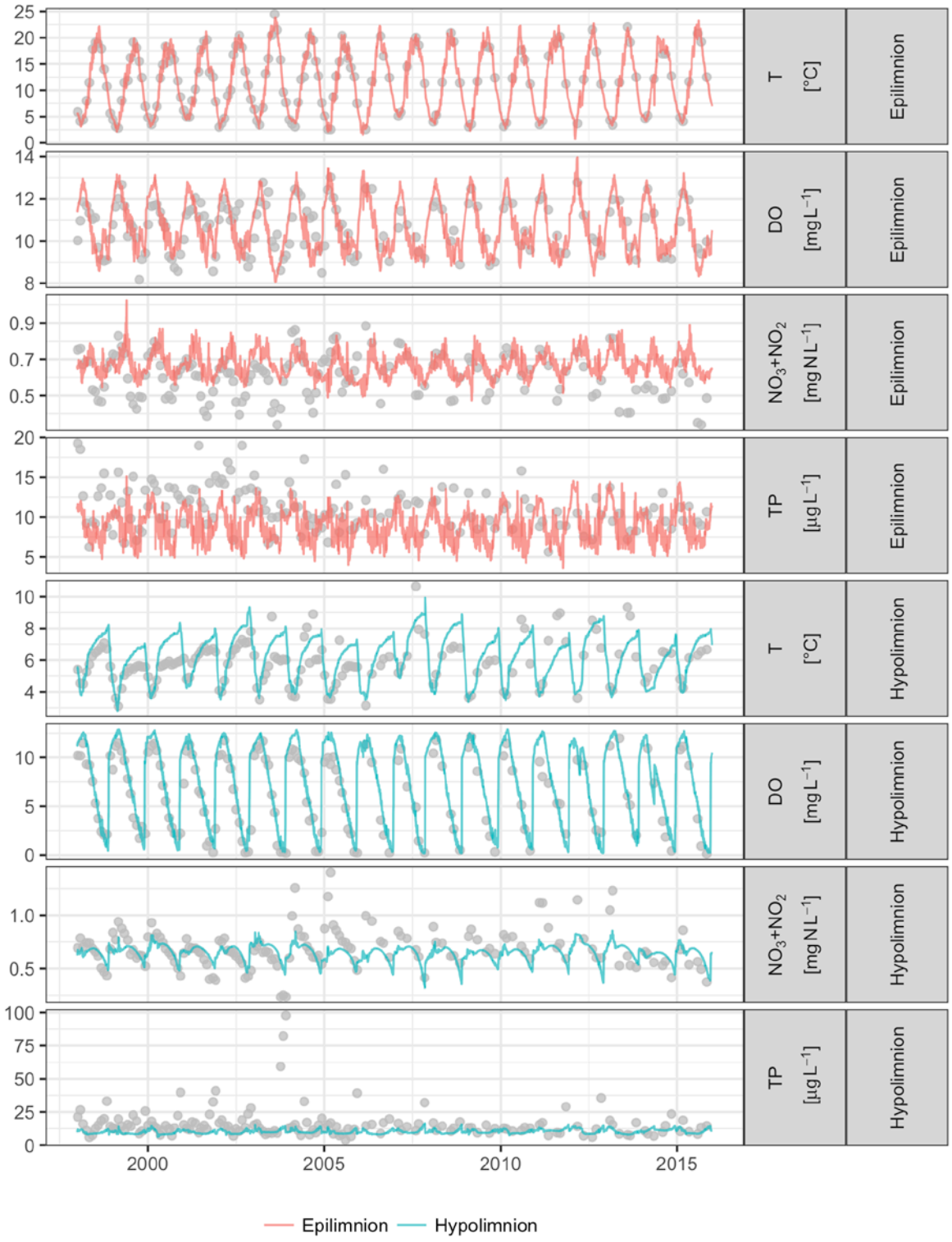

Figure B6. Time series of simulated (lines) and observed (grey points) variables at Upper Lake Zurich; depicted are temperature (T) in °C, dissolved oxygen (DO) in mg L^{-1}, sum of nitrate and nitrite (NO_3+NO_2) in µg N L^{-1} and total phosphorus (TP) in µg P L^{-1} all aggregated volumetrically for either epi- (uppermost 5 m of the water column) or hypolimnion (all depths ≥ 20 m).

C. Results at Upper Lake Zurich

Figure C2 shows the mean and extrema of all considered PS scenarios for Upper Lake Zurich, and Figure C3 shows a boxplot of seasonal differences between either the reference scenario or the extended PS scenario and the present PS scenario. Both figures are separated for epi- and hypolimnion and individually show results for temperature, dissolved oxygen and nutrients.

Effects on temperature in Upper Lake Zurich are minor, with largest deviations in winter (Dec-Feb) due to warmer hypolimnetic water from Sihlsee being released at the surface of Upper Lake Zurich. However, the warming of the entire water column in winter remains at <0.2 °C and <0.5 °C for present PS and extended PS, respectively (Figure C1, Figure C2), since the PS generating flow only accounts to ~10% and ~of natural inflows.

Schmidt stability, which is shown in Figure C3b, is hardly affected due to different PS operations, while the duration of summer stratification lasts ~1 week longer without PS operation, (information is taken from Figure C3a, which shows boxplots of start and end of summer stratification). As a consequence, the dissolved oxygen concentrations in autumn are reduced and the nutrient concentrations are increased without PS operation (Figure C1, Figure C2). The periods with dissolved oxygen concentrations <4 mg L^{-1} span on average ~101, ~100 and ~95 days, for the reference, present PS and extended PS scenarios, respectively. Additionally, the nutrient concentrations of the scenarios with PS are modified by the input of water with different concentrations from the hypolimnion of Sihlsee. Thus, phosphate concentrations are reduced by ~1 and ~2 μg P L^{-1} from November to February for present and extended PS, respectively. The sum of nitrate and nitrite concentrations decrease during the entire year by ~15-50 μg N L^{-1} for both present and extended PS compared to the reference scenario. Between the present and the extended PS scenario the differences remain <15 μg N L^{-1}.

In summary, however, all projected impacts on temperature, stratification, oxygen and nutrient concentrations in Upper Lake Zurich for both the present and the extended PS scenarios do not exceed the interannual variation of these parameters that occur due to variations in meteorology and streamflow. Yet, in the vicinity of the intake/outlet of the PS hydropower plant we cannot exclude the possibility of more relevant effects due to PS operation [16].

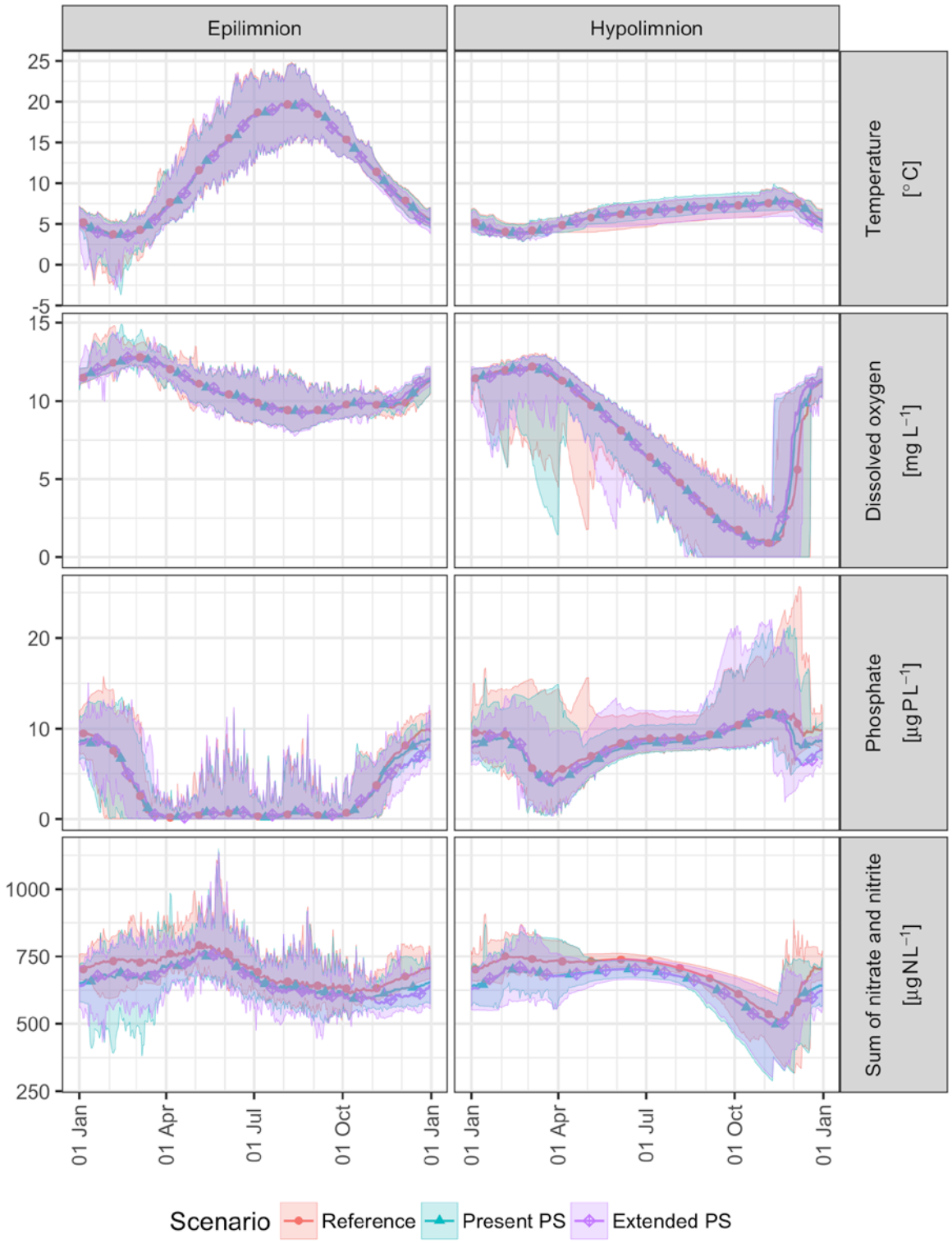

Figure C1. Mean (lines with markers) and range of minima and maxima (shaded areas) of simulated temperature (°C) and concentrations of dissolved oxygen (mg L^{-1}), phosphate (µg P L^{-1}) and the sum of nitrate and nitrite (µg N L^{-1}) for the reference (red), the present PS (green) and the extended PS (blue) scenario at Upper Lake Zurich.

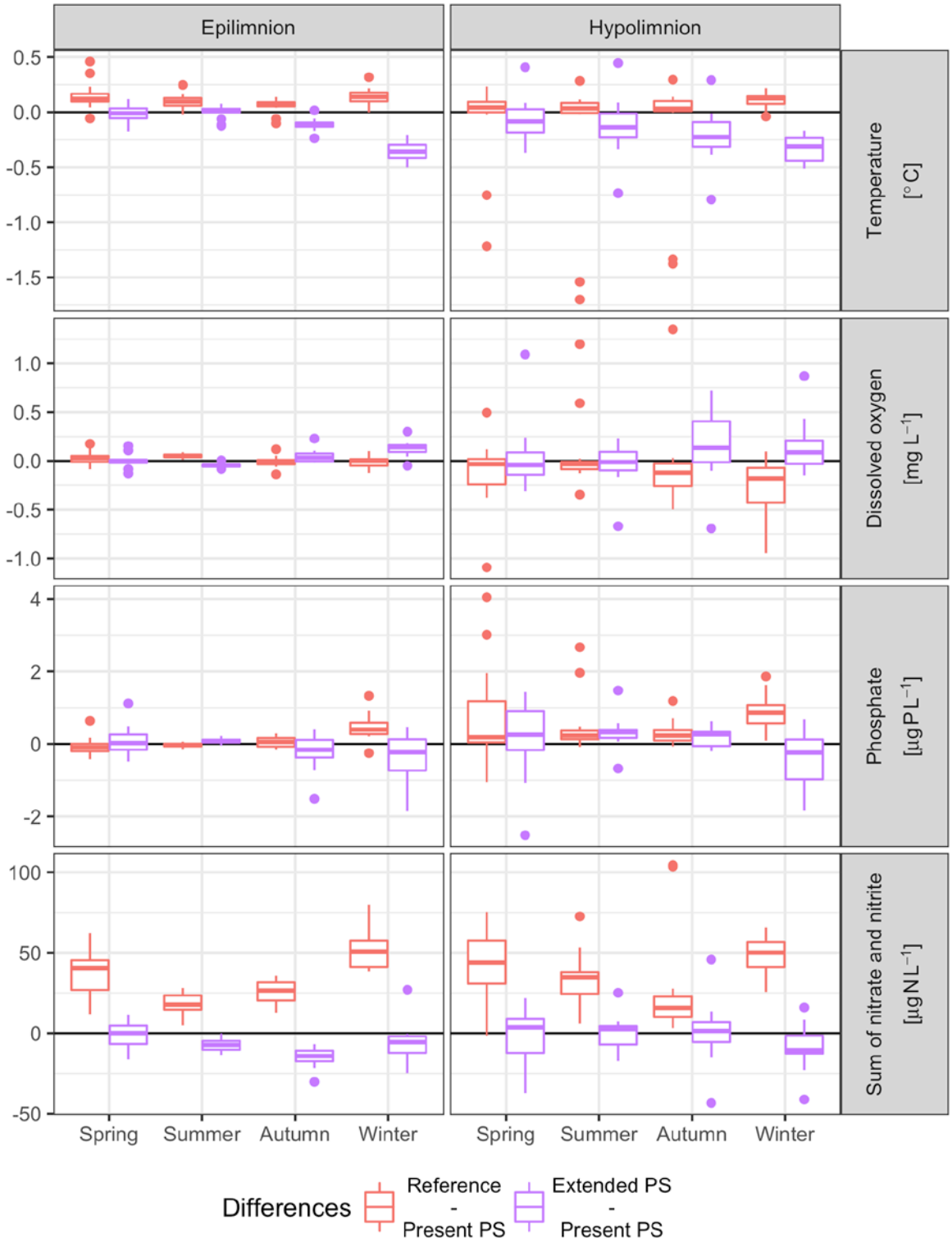

Figure C2. Boxplots of differences in either the reference scenarios or the extended PS scenario to the present PS scenario of temperature (°C) and concentrations of dissolved oxygen (mg L^{-1}), phosphate (µg P L^{-1}) and the sum of nitrate and nitrite (µg N L^{-1}) at Sihlsee. Points show outliers; values were aggregated seasonally for each year before plotting (winter: Dec-Feb, spring: Mar-May, summer: Jun-Aug, autumn: Sep-Nov).

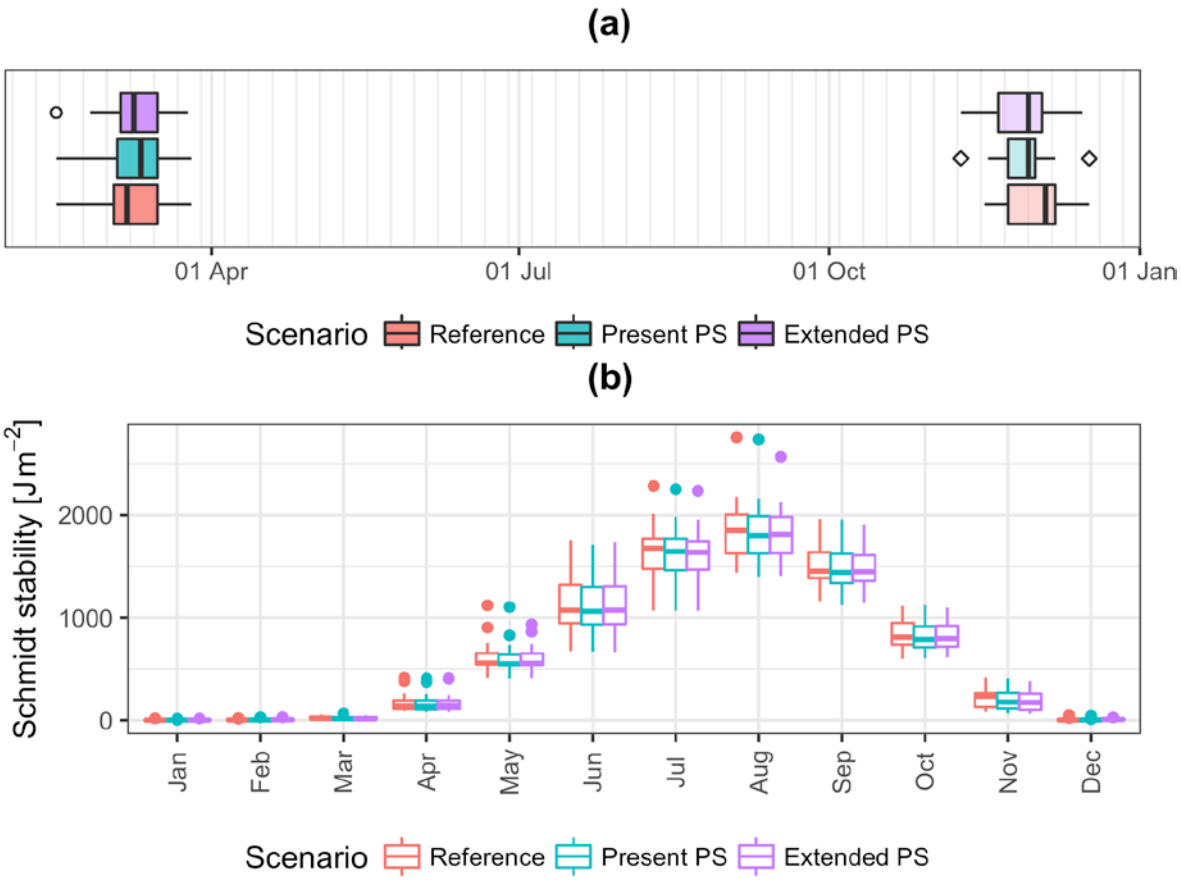

Figure C3. Boxplots for the reference scenario, the present PS and the extended PS scenario at Upper Lake Zurich: (**a**) Start and end of summer stratification; (**b**) Schmidt stability (J m^{-2}), aggregated to monthly mean for each year before plotting. Points show outliers of start (circles) and end (squares) of summer stratification.

D. Specifications of pumped-storage hydropower plants in literature review

Table D1. Specifications of pumped-storage hydropower plants and the connected water bodies (WB) studied in a similar context.

Publication	Head [m]	Volume upper WB [10^6 m^3]	Volume lower WB [10^6 m^3]	Surface area upper WB [km^2]	Surface area lower WB [km^2]	Max. depth upper WB [m]	Max. depth lower WB [m]	Max. PS generation flow [m^3 s^{-1}]	Max. PS pumping flow [m^3 s^{-1}]	Intake/outlet location upper WB	Intake/outlet location lower WB
Bonalumi, *et al.* [14]	~1270	~22	~111	1.43	1.95	26	85	~95	~74	Lower hypolimnion	Upper hypolimnion
Potter, *et al.* [17]	~27	~580 [1]	~407 [1]	~85 [1]	~62 [1]	~33 [1]	~7 [1]	~1347 [2]	~991 [2]	Upper hypolimnion	Upper hypolimnion
USBR [18]	~145	~14	112.6	~1.2 [3]	73	~20 [3]	~27	~112	~97	Lower hypolimnion	Lower hypolimnion
Bermúdez, *et al.* [19]	~283	87 [4]	72 [4]	~7.0	~6.3	~30	~20	~150	~124	Lower hypolimnion	Upper hypolimnion
Anderson [20]	~500	7	74	0.31	13.4	~49	~9	~40	~75		Upper hypolimnion

[1] https://epd.georgia.gov/sites/epd.georgia.gov/files/related_files/site_page/oc5.pdf, 28 February 2018

[2] Estimated with an efficiency of 0.9 and 0.8 for generating and pumping, respectively, from the installed capacities given at http://www.energystorageexchange.org/projects/239, 28 February 2018

[3] https://www.usbr.gov/tsc/techreferences/rec/REC-ERC-82-06.pdf, 28 February 2018

[4] Given is only the storage capacity

References

1. Flerchinger, G.N.; Xaio, W.; Marks, D.; Sauer, T.J.; Yu, Q., Comparison of algorithms for incoming atmospheric long-wave radiation. *Water Resources Research* **2009**, *45*, W03423.

2. Dilley, A.C.; O'Brien, D.M., Estimating downward clear sky long-wave irradiance at the surface from screen temperature and precipitable water. *Quarterly Journal of the Royal Meteorological Society* **1998**, *124*, 1391-1401.

3. Unsworth, M.H.; Monteith, J.L., Long-wave radiation at the ground. *Quarterly Journal of the Royal Meteorological Society* **1975**, *101*, 13-24.

4. Deacon, E.L., The derivation of Swinbank's long-wave radiation formula. *Quarterly Journal of the Royal Meteorological Society* **1970**, *96*, 313-319.

5. Zappa, M.; Andres, N.; Kienzler, P.; Naef-Huber, D.; Marti, C.; Oplatka, M., Crash-Tests for forward-looking flood control in the city of Zürich (Switzerland). *Proc. IAHS* **2015**, *370*, 235-242.

6. Bollrich, G., *Technische Hydromechanik 1*. Verlag Bauwesen: Berlin, **2007**.

7. Keller, H.; Weibel, P., Suspended sediments in streamwater - indicators of erosion and bed load transport in mountainous basins. *IAHS Publication* **1991**, *203*, 53-61.

8. Peters-Kümmerly, B., Untersuchung über Zusammensetzung und Transport von Schwebstoffen in einigen Schweizer Flüssen. *Geographica Helvetia* **1973**, *28*, 137-151.

9. Haynes, W., *CRC Handbook of Chemistry and Physics*. 95 ed.; CRC press.: Boca Raton, FL, **2014**.

10. Gammeter, S.; Forster, R. *Langzeituntersuchungen im Zürichobersee 1972-2000*; Wasserversorgung Zürich: Zürich, **2002**.

11. Der Schweizerische Bundesrat, Gewässerschutzverordnung vom 28. Oktober 1998 (GSchV); SR 814.201; Der Schweizerische Bundesrat: Bern, Switzerland. **1998**.

12. Schildknecht, A.; Köster, O.; Koss, M.; Forster, R.; Leemann, M. *Gewässerzustand von Zürichsee, Zürichobersee und Walensee - Auswertungen der Untersuchungsergebnisse bis 2010, Tech. Bericht der Stadt Zürich*; Wasserversorgung Zürich: Zürich, **2013**.

13. Mieleitner, J.; Reichert, P., Analysis of the transferability of a biogeochemical lake model to lakes of different trophic state. *Ecological Modelling* **2006**, *194*, 49-61.

14. Bonalumi, M.; Anselmetti, F.S.; Wüest, A.; Schmid, M., Modeling of temperature and turbidity in a natural lake and a reservoir connected by pumped-storage operations. *Water Resources Research* **2012**, *48*, WR01184.

15. Mieleitner, J.; Reichert, P., Modelling functional groups of phytoplankton in three lakes of different trophic state *Ecological Modelling* **2008**, *211*, 279-291.

16. Müller, M.; De Cesare, G.; Schleiss, A.J., Flow field in a reservoir subject to pumped-storage operation – in situ measurement and numerical modeling. *Journal of Applied Water Engineering and Research* **2018**, *6*, 109-124.

17. Potter, D.U.; Stevens, M.P.; Meyer, J.L., Changes in physical and chemical variables in a new reservoir due to pumped storage operations. *JAWRA Journal of the American Water Resources Association* **1982**, *18*, 627-633.

18. USBR *Aquatic ecology studies of Twin Lakes, Colorado, 1971-1986: Effects of a pumped-storage hydroelectric project on a pair of montane lakes.*; USBR: Denver, CO, USA, **1993**.

19. Bermúdez, M.; Cea, L.; Puertas, J.; Rodríguez, N.; Baztán, J., Numerical Modeling of the Impact of a Pumped-Storage Hydroelectric Power Plant on the Reservoirs' Thermal Stratification Structure: a Case Study in NW Spain. *Environmental Modeling & Assessment* **2018**, *23*, 71-85.

20. Anderson, M.A., Influence of pumped-storage hydroelectric plant operation on a shallow polymictic lake: Predictions from 3-D hydrodynamic modeling. *Lake and Reservoir Management* **2010**, *26*, 1-13.